Juin 1970

LRP 43/70

CENTRE DE RECHERCHES EN PHYSIQUE DES PLASMAS

FINANCÉ PAR LE FONDS NATIONAL SUISSE DE LA RECHERCHE SCIENTIFIQUE

EXPERIMENTAL INVESTIGATION OF THE 90 MW ROTATING MAGNETIC FIELD PINCH

A. Berney

A. Heym

F. Hofmann

I.R. Jones

LAUSANNE

Juin 1970

LRP 43/70

EXPERIMENTAL INVESTIGATION OF THE 90 MW ROTATING MAGNETIC FIELD PINCH

A. Berney

A. Heym

F. Hofmann

I.R. Jones

Abstract

This paper presents the results and interpretation of measurements made on the 90 MW rotating magnetic field pinch. Three standard filling pressures of 20, 60 and 180 mTorr He were chosen and the following measurements were made: streak and framing photography, electron line density profiles, electron and ion temperatures and detailed magnetic probe measurements.

A possible interpretation of the experimental results leads to the following conclusions:

(i) Under the conditions of 20 and 60 mTorr He filling pressures, the average plasma pressure exceeds that of the confining magnetic field before the end of the experiment. On the contrary, the plasma is magnetically confined throughout the duration of the rotating field pulse in the 180 mTorr case.

(ii) An isotropic, anomalously high value of plasma resistivity has been observed. The existence of conditions favourable to the development of micro-turbulence in the current-carrying boundary layer are inferred from the experimental data.

Lausanne

I. Introduction

The name 'rotating magnetic field pinch' is given to a configuration in which a high-β cylindrical plasma column is confined by a magnetic field having a longitudinal (B_z) and an azimuthal (B_θ) component of identical amplitudes. Both components oscillate at the same fixed frequency but are dephased by 90°. The magnetic field lines on the plasma surface thus change their direction continuously (Fig. 1a). At any given point on the plasma surface, the magnetic field vector rotates in a tangent plane with its tip moving along a circle (Fig. 1b).

The first and foremost reason for studying this configuration is the theoretical one that, given a certain minimum frequency of rotation, the plasma column is positively stable against all macroscopic surface deformations (Weibel 1958, 1959, 1960; Troyon 1967, 1970 a, 1970 b). The actual value of this frequency depends on the choice of plasma model; in general, it is lower for a collision-free plasma column than for a collision - dominated one. For either model, the important assumptions are that the plasma column be surrounded by a conducting shell and that the boundary layer in which the field and the plasma mix be thin. It should further be noted that the rotating field pinch has an equilibrium position, and remains stable, even when produced in a toroidal geometry.

Other advantages of this confinement scheme are the following. Since the magnetic field is confined to a thin boundary layer, loss of energy by cyclotron radiation is minimized. Furthermore, again because the current is concentrated in a thin layer, the current density is very high and so, initially, is the ohmic dissipation. When the mean free path of the charged particles becomes comparable to the width of the field-plasma boundary layer, this ohmic heating ceases to be important. At this time, however, it is possible to change the relative amplitudes of the B_z and B_θ field components so that the plasma surface experiences magnetic pressure variations at twice the rotation frequency. Because of the long mean free path,

these pressure variations are not propagated into the interior of the plasma column as acoustic waves but rather as longitudinal ion oscillations which, as a result of strong ion Landau damping, attenuate within a distance comparable to the plasma radius. This heating mechanism affects the ions only and is very effective (Weibel, 1963). In principle, therefore, the efficient heating of the plasma column of a rotating field pinch presents no problems; it can readily be achieved by means of ohmic heating followed by ion heating.

The main difficulty of producing a rotating field pinch is technological: large magnetic fields (1-5 KGauss) at radio frequencies (1-5 MHz) must be produced. In this laboratory the problem has been resolved (at least to the extent of allowing the theoretical ideas to be tested) by the development of high power pulse generators based on transmission lines of the lumped and continuous varieties (Weibel, 1964; Keller, 1965; Lietti, 1969 a). As a result of this development it has been possible to construct an apparatus capable of generating a rotating field pinch. A description of the apparatus and some very preliminary experimental results have previously been published (Jones et al, 1968). It is the aim of this paper to present the results of measurements which have since been made on the installation.

2. Apparatus

The rotating field pinch is produced by the superposition of an alternating θ-pinch and an alternating Z-pinch (Fig. 1c). A detailed description of the apparatus has already been given; at this time it suffices to list its basic parameters.

Internal diameter of discharge tube, 2 R	=	49 mm
Distance between Z-electrodes, L_o	=	488 mm
Diameter of Z-current return strap	=	65 mm

Maximum amplitude of B_z (B_θ) field at inner wall of discharge tube	=	2.1 (2.3) Kgauss
Frequency of rotation	=	3.1 MHz
Duration of rotating field	=	2·3 μsec (7 periods)

The measurements reported in this paper were made on a modified version of this apparatus. The modifications were mainly concerned with reducing the impurity content of the discharge and included, for example, the substitution of a high purity alumina discharge tube for the original pyrex one, the incorporation of a large liquid nitrogen trap, the use of indium O-rings instead of the previous neoprene ones and the prior cleaning of the discharge tube by means of an R.F glow discharge (Heym, 1968).

The experimental results which follow were obtained using helium as filling gas at initial pressures of 20, 60 and 180 mTorr.

3. Measurements

3.1 Streak and framing photography

Fig. 2 shows axial streak photographs of the rotating field pinch taken at the three standard values of the initial filling pressure. The origin of the time scale below the photographs corresponds to the start of the rotating field discharge. Auxiliary spectroscopic measurements show that the light recorded on the film is mainly due to line radiation of helium and various impurities (mainly oxygen and nitrogen). As will be shown later, there is only a rough correlation between the light and electron density distributions across the discharge tube. Above the streak photograph of Fig. 3 (60 mTorr filling pressure) is shown a row of framing camera pictures. These show that the light emitting region of the plasma retains its cylindrical symmetry throughout the duration of the R.F. pulse.

A comparison of these photographs with the ones published in Jones et al (1968) shows that:

(i) the light intensity in the present streak/framing photographs is about ten times less. In particular, the wall light which appeared towards the end of the implosion stage in the previously published photographs, and which was correlated with "wall-breakdown", is now much reduced.

(ii) the time taken for the light emitting region to reach the discharge tube axis is shorter in the present experiments.

These effects are attributed to a reduced impurity concentration in the modified version of the apparatus.

3.2 Electron line density profiles

The axial electron line density was measured by means of a Mach-Zehnder interferometer (Heym, 1968) which utilizes a He-Ne laser beam. The part of the laser beam which traverses the plasma has a length, L_1, of 408 mm (this being the distance between the "look-ins" described in the above reference) and an effective diameter of 1 mm. The time variation of the axial electron line density, $\bar{n}_e(r,t)$, where

$$\bar{n}_e(r,t) = \frac{1}{L_1} \int_0^{L_1} n_e(r,z,t)\, dz$$

r, θ, z - cylindrical coordinates

n_e - local electron density

was measured with the laser beam located at a fixed radial position. Density profiles were obtained by repeating the measurements at a number of radial positions.

The results of such measurements are shown in Figs. 4, 5 and 6. Each value is the mean of at least three measurements. It is at once evident that there is only a very rough correlation between the density profiles and the distribution of light on the streak picture - the correlation is best for the 180 mTorr He case where the importance of the impurity line radiation is least.

Integration of these density profiles over radius and length gives the total number of electrons, $N_e(t)$, present at each instant in the discharge tube. The variation of N_e with time is shown in Fig. 7 for the three standard filling pressures. In this graph the values have been normalized to that which corresponds to complete double ionization of the filling gas (N_e^*).

3.3 Ion Temperature, T_i

The temperature of the singly-ionized helium ion species was obtained by observing the Doppler broadening of the He II 4686 Å line. The use of a 12-channel Fabry-Perot interferometer (Berney, 1970) enabled the complete line profile to be obtained from a single shot. These measurements were made using an optical system which was sighted along the discharge tube and which accepted axially parallel light coming from a cylindrical region of plasma, length ~ 500 mm and diameter ~ 8 mm. Coarse radial resolution was achieved by observing the line broadening with the axis of this cylindrical region situated at r = 0; 6; 12 and 18 mm.

The measured line widths were corrected for instrumental broadening, Stark broadening (using the results of Section 3.2) and also the effect of reabsorbtion. The resultant corresponding ion temperatures are plotted in Fig. 8. Each value is the average of at least five measurements. It should be pointed out that in certain cases the corrections were so large that only very rough estimates of the ion temperature could be obtained.

3.4 Electron Temperature, T_e

The ratio of the total line and continuum intensities (in 100 Å band centred at the line) for the He II 4686 Å line was measured as a function of time. The measurement was made with no spatial resolution and only for the 60 mTorr He filling pressure case. The variation of the electron temperature, as deduced from this ratio (Griem, 1964), is shown in Fig. 9. The points shown on this graph are the mean values of three measurements.

Care must be taken in the interpretation of these measurements. For the case of a plasma which is undergoing rapid ionization, the population of the upper state of the line may depart considerably from its Saha-Boltzmann value. In addition there may be some uncertainty involved in the experimental measurement of the continuum intensity.

3.5 Magnetic probe measurements

The magnetic field configuration of the rotating field pinch was examined by means of a double magnetic probe which was capable of measuring simultaneously the two field components, B_θ and B_z (Jones et al, 1969). By making measurements with the probe located at various radial positions, it was possible to obtain $B_\theta(r,t)$ and $B_z(r,t)$ with good space and time resolution.

For illustration, a set of instantaneous radial profiles of B_θ are shown in Fig. 10 covering the period t = 1250 ns to 1525 ns in steps of 25 nsec. Each experimental point is the mean of at least four measurements. The entire set of experimental data gave profiles such as these, and corresponding ones for B_z, covering the total duration of the rotating field pinch. Of necessity, the B_θ component falls to zero at the tube axis; it is of interest to note, however, that in the interior region $0 < r < 13$ mm, the B_z and B_θ components were never found to be more than 2% of their surface values.

The components of the electric field are related to the time derivatives of the magnetic induction through the equations:

$$E_\theta(r,t) = \frac{-1}{r} \frac{\partial}{\partial t} \int_o^r r' B_z(r',t)\, dr' \qquad (1)$$

and

$$E_z(r,t) = \frac{\partial}{\partial t} \int_o^r B_\theta(r',t)dr' + E_z(o,t) \qquad (2)$$

For the present experiments, the value of the constant of integration, $E_z(o,t)$, is zero at all times. The values of $E_\theta(R,t)$ and $E_z(R,t)$ were calculated using the above relationships; the maximum values observed were never greater than 100 v/cm.

Knowing the values of $B_\theta(R,t)$, $B_z(R,t)$, $E_\theta(R,t)$ and $E_z(R,t)$, it is possible to calculate the rate of energy flow from the θ - and Z - circuits through the surface A ($= 2\pi RL_o$) defined by the inner wall of the discharge tube

$$P_\theta(t) = \frac{A}{\mu_o} E_\theta(R,t)\, B_z(R,t) \quad ; \quad P_z(t) = \frac{A}{\mu_o} E_z(R,t)\, B_\theta(R,t)$$

These quantities are shown plotted in Fig. 11 a, b for the 60 mTorr He case. The energies, $W_\theta(t)$ and $W_z(t)$, deposited in the discharge tube can be obtained by integrating the corresponding power curves. The result of such integrations is shown in Fig. 11 c, d. The curve in Fig. 11 e shows how the total energy, $W_\theta + W_z$, in the discharge tube increases with time. At the end of the rotating field discharge, 70 joules (64 joules for the 20 mTorr case and 63 joules for 180 mTorr He) have been transferred from the R.F generators to the discharge tube. Since 208 joules were initially stored in the generators, this represents a transfer efficiency of 34 % .

Since a great deal of information is extracted from the magnetic field plots, it was deemed judicious to carry out an independent check on the reliability of the probe measurements. To this end, simultaneous measurements were made of the voltage, $V_z(t)$, between the Z-electrodes and the axial current, $I_z(t)$. These measurements were analysed to give the power flow between the rf Z-generator and the discharge tube and, by integration, the energy $W_z(t)$ entering the discharge vessel. This latter result is shown in Fig. 11 c where it can be compared with that obtained from the probe data. The agreement between these two independent measurements demonstrates, to a large measure, the validity of the magnetic probe data.

The value of the plasma surface resistivity, R_s, (i.e. the resistance of the plasma surface for a unit length and unit width) was obtained by dividing the average power by the mean square current. The following equations were used:

$$R_s(t) = \frac{L_o}{2\pi R} \frac{\overline{P_\theta}(t)}{\overline{I_\theta^2}(t)}$$

and

$$R_s(t) = \frac{2\pi R}{L_o} \frac{\overline{P_z}(t)}{\overline{I_z^2}(t)}$$

where the bar indicated a suitably time-averaged quantity (see, for example, Fig. 11 a,b). Values of R_s thus obtained for the three standard filling pressures are shown in Fig. 12 a, b, c. Lietti (1969 b) has independently determined average values of R_s; these are indicated in Fig. 12. These values were obtained by comparing the actual performance of the rf θ-generator with that it had when loaded with a circuit consisting of a fixed inductor (to simulate the plasma inductance) and a known, fixed resistor.

4. Discussion of Results

Due to the absence of reliable temperature measurements having good space resolution - especially in the neighbourhood of the discharge tube wall where most of the current flows - any interpretation of the experimental data must, of necessity, be a tentative one.

An interpretation based on certain reasonable hypotheses has been made. Quantitative conclusions regarding the containment and resistivity of the plasma have been reached; these are discussed in paragraphs 4.1 - 4.3.

4.1 Excess Electrons

Despite the efforts made to reduce the impurity content of the discharge, the results shown in Fig. 7 indicate the presence of an excess of electrons in the discharge tube. For two of the curves (20 and 60 mTorr He), the value of $N_e(t)/N_e^*$ rises above that corresponding to complete double ionization of the filling gas. If, for the moment, we ignore the second rise which occurs towards the end of the discharge in the 20 mTorr He case, it is possible to identify final, steady values of N_e/N_e^* which are indicated in Fig. 7 by dashed lines. The fractional increase of this final value, compared to the expected value of unity, is inversely proportional to the filling pressure. This implies that a constant excess number of electrons are generated in the tube whatever the value of the initial filling pressure. This excess number of electrons is evaluated to be $5{\cdot}9 \times 10^{17}$ electrons. The origin of these excess electrons is unknown; they could arise from the ionization of impurities (O_2 and N_2) in the filling gas, from sputtering of the aluminium Z - electrodes, from the ionization of an adsorbed layer of helium atoms or from error in the measurement of the filling pressure. While probably all of these mechanisms are involved, it is assumed in the following discussion that the excess electrons originate from the ionization of additional helium atoms.

4.2 Plasma Confinement

An estimate of the average plasma pressure can be made as follows. Let

$N(t)$ = total number of neutral helium atoms in the discharge tube at time t

$N_e(t)$ = total number of electrons in the discharge tube at time t

N_f = final total number of electrons in the discharge tube (the value corresponding to the dashed line in Fig. 7)

$N^+(t)$ = total number of singly ionized helium ions in the discharge tube at time t

$N^{++}(t)$ = total number of doubly ionized helium ions in the discharge tube at time t

$\alpha(t)$ = $N_e(t)/N_f$

$W(t) = W_\theta(t) + W_z(t)$ = total energy dissipated in the discharge tube during the interval $0 < t' < t$

$W_{th}(t)$ = thermal energy of the plasma at time t

$W_i(t)$ = total energy used for ionization during the interval $0 < t' < t$

$p(t) = \frac{2}{3}\frac{W_{th}(t)}{V}$ = average plasma pressure where V is the volume of the discharge tube

$p_m(t) = \frac{1}{2\mu_o}\overline{B_\theta^2(R,t) + B_z^2(R,t)}$ = average magnetic pressure at the inner wall of the discharge tube

ε_1 = first ionization potential of helium (= 24·6 eV)

ε_2 = second ionization potential of helium(= 54·4 eV)

We assume that of the three species N, N^+ and N^{++}, only two, namely (N, N^+) or (N^+, N^{++}), co-exist at any given time.

When $N_e < N_f/2$ (i.e $\alpha < 0{\cdot}5$), we suppose that

$$N = N_f/2 - N_e$$

$$N^+ = N_e$$

$$N^{++} = 0 \ ,$$

whence

$$W_i = N_e \varepsilon_1 e$$
$$= \alpha N_f \varepsilon_1 e$$

When $N_e > N_f/2$ (i.e $\alpha > 0{\cdot}5$) ,

$$N = 0$$

$$N^+ = N_f - N_e$$

$$N^{++} = N_e - N_f/2$$

and it follows that

$$W_i = N^+ \varepsilon_1 e + N^{++}(\varepsilon_1 + \varepsilon_2)\, e$$

$$= N_f e \{\alpha \varepsilon_2 - \frac{1}{2}(\varepsilon_2 - \varepsilon_1)\}$$

Calculation shows that the loss of energy by bremsstrahlung, radial thermal conduction and axial mass flow is negligible during the duration of the rotating field pinch. In addition, the amount of energy in the form of kinetic energy is at all times small in comparison with W(t). It is difficult to estimate the loss of energy by axial thermal conduction. If, however, we assume that this is also an unimportant loss mechanism during the 2.3 μsec duration of the experiment, we can write

the following energy balance equation:

$$W_{th}(t) = W(t) - W_i(t) + \left[W_{th} + W_i \right]_{t = 0}$$

where the quantity in square brackets can be evaluated from a knowledge of the initial degree of ionization and from a reasonable estimate (2eV) of the preionized plasma temperature. Knowing the experimentally determined quantities, $W(t)$, N_f and α, it is possible to calculate $W_{th}(t)$ and hence the average plasma pressure, $p(t)$. The time variation of $p(t)$ was calculated for the three standard experimental conditions; the results are shown in Table 1 (60 mTorr He case only) and Fig. 13 where the ratio $p(t)/p_m(t)$ is plotted.

If the ratio $p(t)/p_m(t) < 1.0$, the plasma is magnetically confined. If, on the other hand, this ratio is greater than unity, then one can only have, at best, an inertial confinement of the plasma during the initial, dynamic phase of the pinch. Once this phase of the discharge has been passed through and a steady state has been achieved, the plasma will be only partially confined by the magnetic field and thermal contact will be established between the plasma and the wall.

The results shown in Fig. 13 indicate that for the 20 and 60 mTorr He cases, the rate of plasma heating is such that before the end of the discharge, the plasma is no longer confined magnetically. For the 180 mTorr He case, however, the plasma remains magnetically confined throughout the duration of the R.F pulse.

The thermal energy, W_{th}, of the plasma decreases with increasing filling pressure and is an immediate consequence of the fact that, whereas the input energy remains approximately constant for all the experimental conditions studied, ionization represents an energy sink which increases with filling pressure. It is of interest to note that the second rise in the 20 mTorr He curve of Fig. 7 occurs when the plasma, no longer magnetically confined, starts to make appreciable thermal contact with the wall

(see, for example, the density profile at 1.8 μsec for the 20 mTorr He case, Fig. 4). It is reasonable to suppose that the excess electrons associated with this second rise results from the interaction of the energetic plasma with the wall. For the 60 mTorr He filling pressure, the plasma is less energetic and does not make thermal contact with the tube wall until later on in the discharge. The second rise in electron density at late times is thus less noticeable.

4.3 Electrical Resistivity

The magnetic field measurements were found to be well represented by expressions of the following form:

$$B_{\substack{\theta \\ z}}(r,t) = B_o e^{-\frac{(R-r)}{\delta}} \begin{matrix} \sin \\ \cos \end{matrix} \left[\omega t - \frac{(R-r)}{\varepsilon} \right]$$

where R is the internal radius of the discharge tube and δ and ε are fitted parameters which are considered to be constant over the depth of the skin layer. The magnetic probe data for the 60 mTorr He experiments was analysed to yield values of δ and ε. The values of ε were determined by following the trajectories of successive zero-crossings of the magnetic field components as they propagated into the plasma while values of δ were obtained from the variation of the magnetic field modulus with radius (see Figs. 10 and 14). These values are thus time - averaged over an interval which is roughly equal to the time taken for a typical field zero-crossing to traverse the skin layer, namely ~ 150 nsec. Both the B_θ and B_z data were used to obtain the time dependence of δ and ε shown in Fig. 15.

The interpretation of Fig. 15 is facilitated if we first calculate the penetration of the electromagnetic field into the plasma in the rotating magnetic field pinch. We examine a simple model having the following properties:

(i) We consider a plane geometry and assume that the plasma occupies the half-space $x > 0$ with the $y - z$ plane coinciding with the plasma surface.

(ii) The plasma moves with a constant velocity, v, in the positive x - direction. To satisfy the equation of continuity at the origin, a plasma source at $x = o$ is assumed.

(iii) The plasma resistivity is anisotropic with respect to the direction of the magnetic field vector. The plasma is assumed to obey an Ohm's law which, in component form, can be written:

$$j_{\parallel} = \frac{E_{\parallel}}{\rho_{\parallel}}$$

$$j_{\perp} = \frac{1}{\rho_{\perp}} (E_{\perp} - vB)$$

(The symbols $\parallel$ and $\perp$ refer to directions parallel and perpendicular to $\vec{B}$)

$\rho_{\parallel}$ and $\rho_{\perp}$ are assumed to be constant in space and time.

If we neglect the displacement current in Maxwell's equations, then it is possible to derive the following steady-state field distribution equations for an imposed rotating field

$$B(0,t) = B_o e^{i\omega t}$$

$$\left[B_y = \mathrm{Re}(B) \quad ; \quad B_z = \mathrm{Im}(B) \right]$$

at the plasma surface.

$$B(x,t) = B_o e^{-\frac{x}{\delta}} e^{i(\omega t - \frac{x}{\varepsilon})}$$

$$E(x,t) = E_o e^{-\frac{x}{\delta}} e^{i\left[\omega t - \frac{x}{\varepsilon} - (\alpha+\beta)\right]}$$

$$j(x,t) = j_o e^{-\frac{x}{\delta}} e^{i\left[\omega t - \frac{x}{\varepsilon} - \beta\right]}$$

where $$E_o = \frac{B_o}{\mu_o}\sqrt{\frac{\rho_{\parallel}^2}{\varepsilon^2} + \left[\frac{\rho_{\perp}}{\delta} + \mu_o v\right]^2}$$

$$j_o = \frac{B_o}{\mu_o}\sqrt{\frac{1}{\delta^2} + \frac{1}{\varepsilon^2}}$$

$$\tan\beta = \frac{\varepsilon}{\delta}$$

$$\tan\alpha = \frac{\left[\rho_{\perp} - \rho_{\parallel} + \mu_o v\delta\right]}{\left[\rho_{\parallel}\frac{\delta}{\varepsilon} + \rho_{\perp}\frac{\varepsilon}{\delta} + \mu_o v\varepsilon\right]}$$

and where δ and ε satisfy the pair of equation:

$$\frac{1}{\mu_o \varepsilon\delta}\left(\rho_{\perp} + \rho_{\parallel}\right) + \frac{v}{\varepsilon} = \omega$$

$$\frac{1}{\mu_o}\left(\frac{\rho_{\parallel}}{\varepsilon^2} - \frac{\rho_{\perp}}{\delta^2}\right) - \frac{v}{\delta} = 0$$

The relative orientation of $\vec{B}$, $\vec{j}$ and $\vec{E}$ in any x = const. plane is shown in Fig. 16.

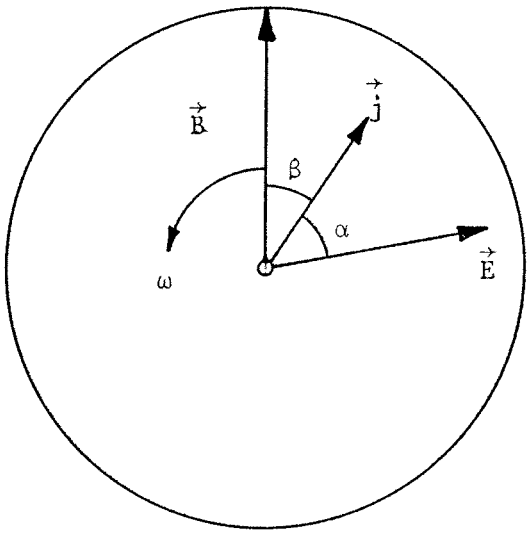

Fig. 16 Relative Orientation of $\vec{B}$, $\vec{j}$ and $\vec{E}$

We proceed to identify three special cases:

I $\rho_{\parallel} = \rho_{\perp} = \rho$ (say) and $v = o$

It follows that $\delta = \varepsilon = \sqrt{\frac{2\rho}{\omega\mu_o}}$ and that

$\alpha = 0$ and $\beta = \pi/4$. This is the usual skin effect result.

II $\rho_{\parallel} \neq \rho_{\perp}$ and $v = o$

In this case:

$$\frac{1}{\delta} = \sqrt{\frac{\omega\mu_o}{2(\rho_{\parallel}\rho_{\perp})^{\frac{1}{2}}} \cdot \frac{2}{(1 + \frac{\rho_{\perp}}{\rho_{\parallel}})}}$$

$$\frac{1}{\varepsilon} = \sqrt{\frac{\omega\mu_o}{2(\rho_{\parallel}\rho_{\perp})^{\frac{1}{2}}} \cdot \frac{2}{(1 + \frac{\rho_{\parallel}}{\rho_{\perp}})}}$$

$$\tan\beta = \sqrt{\frac{\rho_{\parallel}}{\rho_{\perp}}}$$

and $$\tan\alpha = \frac{(\frac{\rho_{\perp}}{\rho_{\parallel}} - 1)}{2\sqrt{\frac{\rho_{\perp}}{\rho_{\parallel}}}}$$

In Fig. 17, values of δ and ε, normalized to the quantity $\left[\frac{2(\rho_{\parallel}\rho_{\perp})^{\frac{1}{2}}}{\omega\mu_o}\right]^{1/2}$ are plotted as a function of the ratio $\rho_{\perp}/\rho_{\parallel}$. It is evident that anisotropy in the plasma resistivity affects δ far more than it does the value of ε.

III $\rho_{\parallel} = \rho_{\perp} = \rho$ and $v \neq 0$

In this case:

$$\frac{1}{\delta} = \frac{\omega}{v_{ph}} (\Delta - V)$$

$$\frac{1}{\varepsilon} = \frac{\omega}{v_{ph}} \cdot \frac{1}{\Delta}$$

$$\tan \beta = \Delta(\Delta - V)$$

$$\tan \alpha = V\Delta$$

where $$\Delta = \left[\left(1 + \frac{V^4}{4}\right)^{\frac{1}{2}} + \frac{V^2}{2} \right]^{\frac{1}{2}}$$

$$V = \frac{v}{v_{ph}}$$

and

$$v_{ph} = \sqrt{\frac{2\omega\rho}{\mu_o}}$$

Values of δ and ε, normalized to the classical skin depth $\sqrt{\frac{2\rho}{\omega\mu_o}}$, are shown plotted as a function of V in Fig. 18. We note that δ is influenced more than ε by the presence of plasma motion.

Turning now to the experimental data presented in Fig. 15, it is possible to clearly distinguish two time domains: the first 1.5 μsec of the pinch when $\delta = \varepsilon$ and the final 0.7 μsec when δ is larger than ε .

<u>0 < t < 1.5 μsec</u>

During this time interval $\delta = \varepsilon$ and, on the basis of the above analysis (Case I), it is concluded that plasma motion and anisotropy of the plasma resistivity are negligible throughout this period of the discharge.Values of the isotropic resistivity, ρ, can be obtained from the experimentally determined values of surface resistivity (Fig. 12) by means of the well-known relationship, $\rho = R_s \delta$. Values so obtained for the 60 mTorr He experiment are shown plotted as a function of time in Fig. 19. We note, in passing, that the application of a plane model to the experimental situation is justified inasmuch as the measured radial extent of the field-plasma boundary is much smaller than the radius of the discharge tube. Furthermore,

the slow variation of ρ with time permits the use of a steady-state theory.

The isotropy of the plasma resistivity was confirmed by rough measurements made of the parallel component, $\rho_{\parallel}$. The values of $E_\theta(r,t)$ and $E_z(r,t)$ were obtained from the magnetic probe data by means of equation (1) and (2). The components of the current density are given by:

$$j_\theta(r,t) = -\frac{1}{\mu_o}\frac{\partial B_z}{\partial r}$$

and

$$j_z(r,t) = \frac{1}{\mu_o r}\frac{\partial}{\partial r}(rB_\theta)$$

The components E_θ, E_z, j_θ and j_z were evaluated for the 60 mTorr He case and were resolved into $E_\perp$, $E_\parallel$, $j_\perp$ and $j_\parallel$. The ratio

$$\rho_\parallel(r,t) = \frac{E_\parallel(r,t)}{j_\parallel(r,t)}$$

was then calculated as a function of time for various radial positions.

It was found that the value of ρ (which, we recall, is assumed to be constant over the full extent of the skin layer) could justifiably be equated to the mean value of the parallel resistivity in the field - plasma boundary. It is reasonable to conclude that for the time interval under discussion, little or no anisotropy of the plasma resistivity has been observed in the 60 mTorr He experiments.

The question remains as to whether of not the measured isotropic plasma resistivity is classical or anomalous. A partial answer can be obtained by means of the following argument. The classical value of the resistivity is given by

$$\rho = \left(\frac{m_e}{e^2}\right)\frac{1}{n_e \tau_{ei}}$$

where τ_{ei}, the collision time for each electron $= \dfrac{2{\cdot}76 \times 10^5 (T_e)^{3/2}}{Z_i^2 \, n_i \, \ell n \, \Lambda}$

(Braginskii, 1958)

If (i) we take the measured value of ρ from Fig. 19

(ii) we calculate the average density, $\bar{n}_e$, in the region 20 mm < r < 24.5 mm from the experimentally determined electron density profiles

(iii) we assume that the helium atoms are at all times doubly ionized in the boundary layer i.e. $\bar{n}_i = \dfrac{\bar{n}_e}{2}$; $Z_i = 2$

and (iv) we assume $\ell n \, \Lambda = 10$

then, by using the above equations, we can construct Table II. It should be emphasized that the quantity T_e is the average electron temperature in the skin layer obtained by assuming that the plasma resistivity is classical

Previous calculation (Table I) has furnished values of the thermal energy of the plasma as a function of time. If it is assumed that this energy is shared equally amongst all the charged particles in the discharge tube, an average temperature, T_{av}, can be calculated. This quantity is also listed in Table II and is seen to be greater than or approximately equal to T_e. Since all the input energy into the discharge tube is originally deposited in the skin layer and since it takes at least a few microseconds for this energy to be distributed equally throughout the tube and amongst all the various charged particle species, it is plausible to conclude that the average plasma temperature in the skin must be much higher than that listed under T_{av} in Table II. This being the case, the disparity which now appears between the electron temperature as estimated from classical resistivity and that obtained from energy considerations can only be resolved by assuming that the resistivity is indeed anomalous in the present experiments. Of course, this argument loses its force if the loss of energy by axial thermal conduction is, in reality, substantial during the time of the rotating field pinch.

The occurrence of anomalously high resistivity in pinch experiments has already been amply reported in the literature (see, for example, Bodin, 1969) and has, in general, been attributed to an enhancement in electron scattering due to the presence of microscopic plasma instabilities. One of the conditions for the onset of microscopic instability is that the ratio of the electron-ion drift velocity $v_D (= j/n_e e)$ to the ion sound speed

$$v_s = \sqrt{\frac{k(Z_i T_e + T_i)}{m_i}}$$

is greater than unity. In order to evaluate this ratio in the present experiments, consider, for example, the conditions in the skin layer at time $t = 1.2$ μsec in the 60 mTorr He discharge. The average values of the current and electron densities are 3.2×10^7 amp/m^2 and 3×10^{20}/m^3 respectively. If now we make the opposite assumption to that made earlier and suppose that the thermal energy resides only in the skin layer, a maximum average skin temperature of $T_{av} = T_e = T_i \sim 6 \times 10^6$ °K is obtained. Hence, at this particular time in the rotating field discharge, the ratio $v_D/v_s > 3.5$. Similar calculations show that $v_D/v_s > 1$ throughout the duration of the pinch (Table III). Since the energy equipartition time between electrons and ions is a few microseconds for the conditions of the experiment, it is very likely that $T_e/T_i > 1$ in the skin layer. This is also a condition which favours the excitation of micro-instability in the current carrying layer.

1.5 μsec < t < 2.2 μsec

During this time interval δ increases to nearly twice its previous value while the value of ε remains sensibly the same as before. This behaviour is consistent with the assumption that at this late stage of the pinch, plasma motion and/or anisotropic plasma resistivity start to play a significant role in the penetration of electromagnetic fields into the plasma. It is not possible to identify which of the two mechanisms predominates ;

it is plausible, however, to assume that it is a velocity effect since it seems improbable that the plasma resistivity would suddenly become anisotropic.

4.4 Magnetic Shear

The magnetic probe data shows that the skin layer possesses magnetic shear. It is reasonable to expect that this shear enhances the stability of the rotating field pinch above the level predicted by Weibel and Troyon who assumed an infinitely thin skin layer in their analyses (see Tuck, 1958).

Measurement of the magnetic shear present in these experiments gave values which were typically between 4.0 - 8.0 radians/cm for the rate of change of pitch angle with radial distance from the discharge tube wall.

4.5 Ion Heating

Mention was made in the introduction to this paper of the possibility of a heating mechanism which affects only the ions and which can be excited by making the polarization of the rotating field elliptic. In practice, the polarization of the magnetic field is elliptic (see, for example, Fig. 7 d of Jones et al, 1968); it is technically very difficult to avoid having some modulation of the magnetic pressure. Thus, if the conditions in the vicinity of the tube wall are favourable (i.e ion mean free paths and cyclotron radii are long in comparison to the depth over which the oscillating magnetic pressure is acting), ion heating of the type described should occur in these experiments.

The magnetic probe date was treated to yield the detailed variation, in space and time, of the magnetic pressure. The sequence of graphs shown in Fig. 20 covers one modulation period and demonstrates convincingly the existence of a magnetic piston which acts on the plasma surface at twice the rotation frequency.

5. Conclusions

The main results of the experiment described in Jones et al (1968) and in the present paper are summarized as follows:

(i) The technical feasibility of generating a rotating magnetic field pinch has been demonstrated.

(ii) In the 20 and 60 mTorr He experiments, it is found that after an initial, transient phase during which the plasma is inertially confined, the plasma pressure attains a value greater than that of the confining magnetic field. Thus the plasma is not magnetically confined under these conditions. On the contrary, the plasma is magnetically confined for the total duration of the rotating field pinch in the 180 mTorr He case.

(iii) During the first 1.5 μsec of the 60 mTorr He rotating field pinch, the plasma resistivity in the skin layer is isotropic and has an anomalously high value. The occurrence of two conditions, $v_D/v_s > 1$ and $T_e/T_i > 1$, which favour the growth of micro-instabilities in the current carrying skin layer are inferred from an analysis of the experimental data. At this time, we are unable to identify the mechanism responsible for the enhanced resistivity.

(iv) During the latter stage of the pinch ($t > 1.5$ μsec) there is a momentary, enhanced penetration of the magnetic field into the plasma which could be due to plasma motion and/or anisotropy of the plasma resistivity. At the end of the discharge the field penetration is once more that found during the early stages of the pinch ((iii) above).

We wish to re-emphasize that the above interpretation of the experimental data is tentative. More definitive conclusions should result from an experiment which is currently underway and which includes the measurement of electron temperature by means of Thomson scattering.

A c k n o w l e d g e m e n t s

The authors gratefully acknowledge the assistance of Dr. A. Lietti and J.-M. Aeschlimann, P. Hafner, J.-P. Perotti and H. Ripper in the construction, maintenance and use of the experimental apparatus. They thank Prof. R. Keller, Prof. E.S. Weibel and Dr. F.S. Troyon for many fruitful discussions.

References

BERNEY A. (1970) Ph.D Thesis, Plasma Physics Centre, Lausanne, Report LRP 40-70

BODIN H.A.B., McCARTAN J., NEWTON A.A. and WOLF G.H. (1969) Plasma Physics and Controlled Nuclear Fusion Research, Vol II, p. 533, International Atomic Energy Agency, Vienna

BRAGINSKII S.I. (1958) Sov. Phys. JETP 6, 358

GRIEM H.R. (1964) Plasma Spectroscopy, McGraw-Hill Book Company, New York, p. 283

HEYM A. (1968) Plasma Phys. 10, 1069

JONES I.R., LIETTI A. and PEIRY J.-M. (1968) Plasma Phys. 10, 213

JONES I.R., PEIRY J.-M. and COCQ D. (1969) Rev. Scient. Instrum. 40, 133

KELLER R. (1965) Helv. phys. Acta 38, 328

LIETTI A. (1969a) Rev. Scient. Instrum. 40, 473

LIETTI A. (1969b) Mesures de résistance de surface dans une expérience de striction par champ tournant de 3 MHz
Plasma Physics Centre, Lausanne, Report Int. 14/69

TROYON F.S. (1967) Physics Fluids 10, 2660

TROYON F.S. (1970a) A numerical study of the stability of a collisionless plasma confined by a rotating magnetic field,
Plasma Physics Centre, Lausanne
Report LRP 41-70

TROYON F.S. (1970b) Study of short wavelength instabilities in the confinement of a collision dominated plasma by a rotating magnetic field,
Plasma Physics Centre, Lausanne
Report LRP 42-70

TUCK J.L. (1958) Proceedings of the Second International Conference on the Peaceful Uses of Atomic Energy,
Geneva, Vol. 32, p. 3.United Nations

WEIBEL E.S. (1958) Proceedings of the Second International Conference on the Peaceful Uses of Atomic Energy,
Geneva, Vol. 32, p. 161. United Nations

WEIBEL E.S. (1959) On the dynamic stabilization of a plasma column,
Space Technology Laboratories,
Los Angeles, Report PRL - 9 - 31

WEIBEL E.S. (1960) Physics Fluids 3, 946

WEIBEL E.S. (1963) Heating and confinement of a plasma by alternating magnetic fields
Plasma Physics Centre, Lausanne
Report LRP 3-63

WEIBEL E.S. (1964) Rev. Scient. Instrum. 35, 173

60 mTorr He

$V = 0{\cdot}92 \times 10^{-3} m^3$

$N_f = 4.30 \times 10^{18}$ electrons

$\left[W_{th} + W_i\right]_{t=o} = 4.4$ joules

t (μsec)	α	W (joules)	W_i (joules)	W_{th} (joules)	p (10^3 n/m^2)	p_m (10^3 n/m^2)
0.4	0.21	2.2	3.6	3.0	2.1	3.4
0.5	0.23	3.9	3.9	4.4	3.1	5.2
0.6	0.25	6.4	4.2	6.6	4.8	7.0
0.7	0.28	8.5	4.7	8.2	5.9	9.4
0.8	0.35	12.9	5.9	11.4	8.3	11.6
0.9	0.42	16.8	7.2	14.0	10.1	13.8
1.0	0.51	22.3	8.7	18.0	13.1	14.5
1.1	0.58	26.0	11.2	19.2	13.9	14.0
1.2	0.73	31.0	17.0	18.4	13.3	13.2
1.3	0.83	33.8	20.8	17.4	12.6	12.2
1.4	0.95	37.3	25.3	16.4	11.9	13.0
1.5	1.0	41.0	27.2	18.2	13.2	14.8
1.6	1.0	45.4	27.2	22.6	16.4	16.9
1.7	1.0	51.1	27.2	28.3	20.5	17.1
1.8	1.0	54.9	27.2	32.1	23.3	15.9
1.9	1.0	62.2	27.2	39.4	28.6	14.8
2.0	1.0	64.1	27.2	41.3	30.0	13.6

T A B L E I

60 mTorr He

t (μsec)	ρ (10^{-4} -m)	$\bar{n}_e$ (10^{21} m^{-3})	τ_{ei} (10^{-10} sec)	T_e (10^4 ^oK)	T_{av} (10^4 ^oK)
0.4	1.00	0.4	8.9	8.7	7.8
0.6	0.81	0.8	5.5	10.0	15.0
0.8	0.78	1.2	3.8	10.3	18.4
1.0	0.70	1.2	4.2	11.0	20.1
1.2	0.60	0.3	19.8	12.3	16.9
1.4	0.48	0.15	49.4	14.2	12.7

T A B L E II

60 mTorr He

t (μsec)	v_D / v_s
0.4	3.9
0.6	2.6
0.8	2.1
1.0	1.9
1.2	3.5
1.4	5.2
1.6	3.1
1.8	1.6
2.0	0.9

T A B L E III

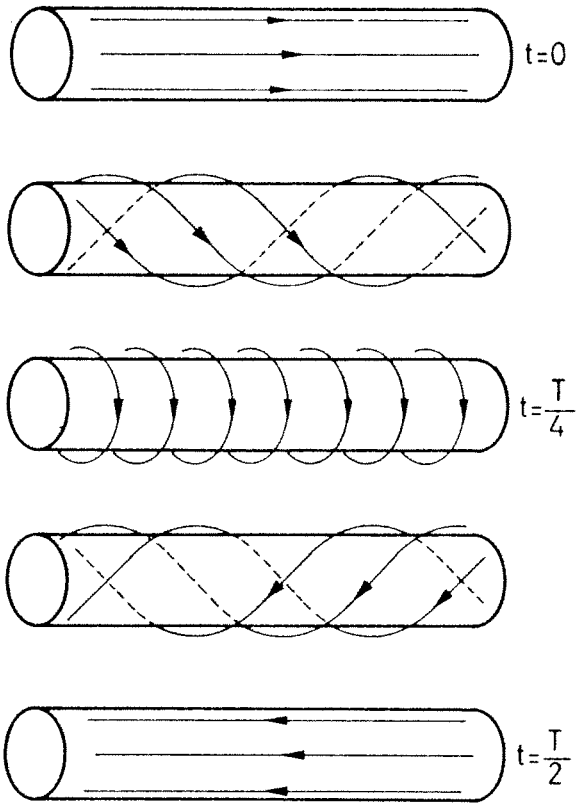

FIG. 1.a) THE MAGNETIC FIELD CONFIGURATION

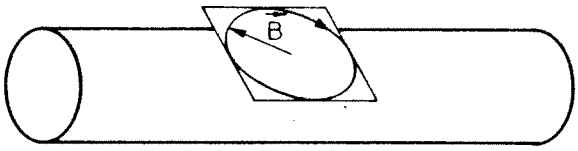

FIG. 1.b) THE MAGNETIC VECTOR AT ANY POINT OF THE SURFACE ROTATES IN A TANGENT PLANE

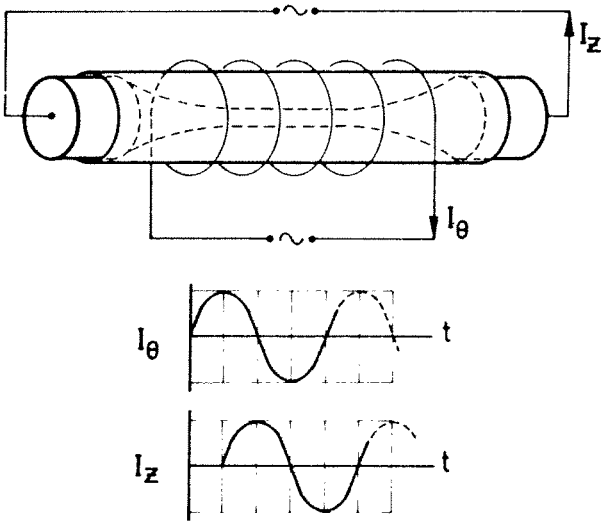

FIG. 1.c) PRACTICAL REALISATON OF THE ROTATING MAGNETIC FIELD PINCH

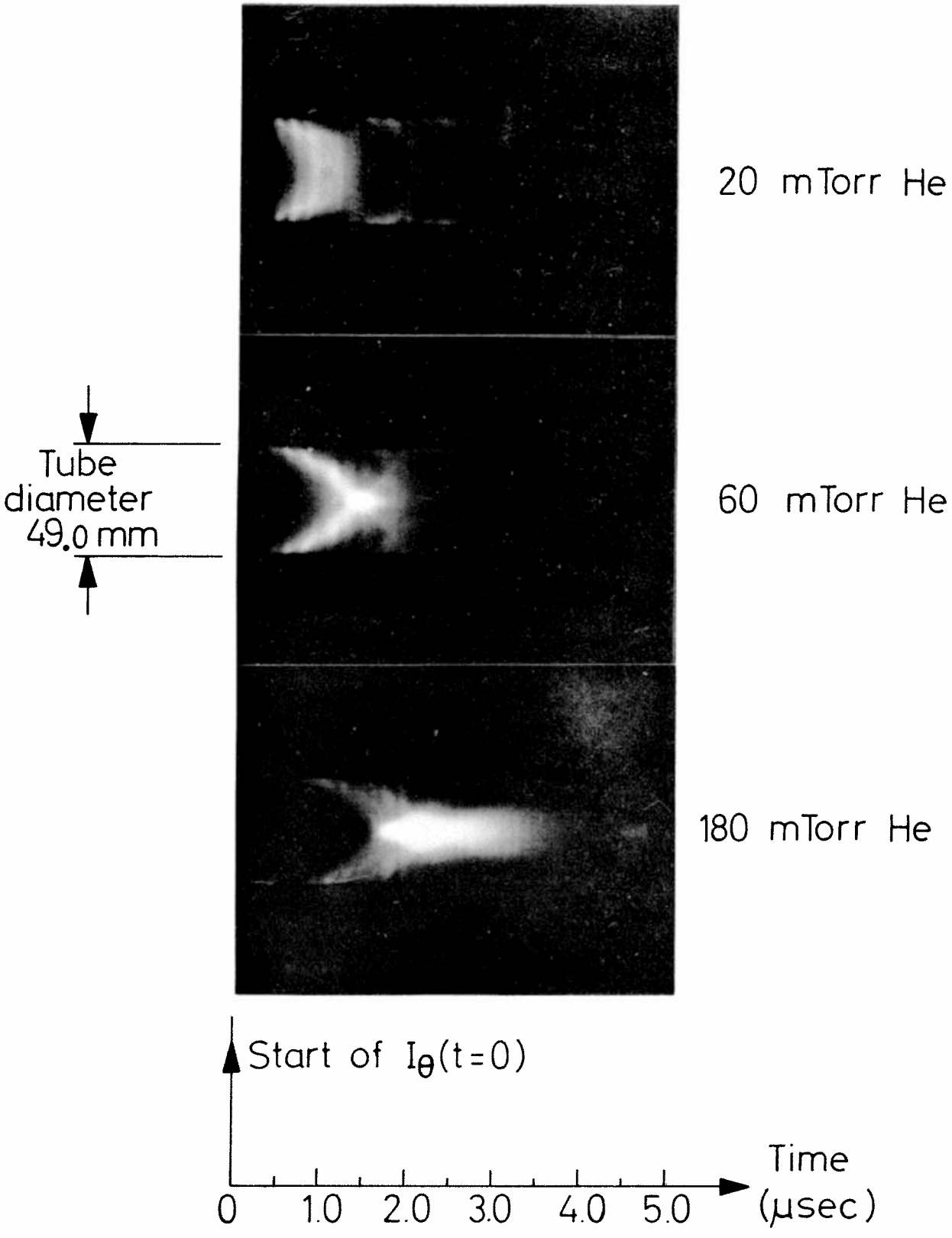

Fig. 2

Streak photographs of the rotating field pinch

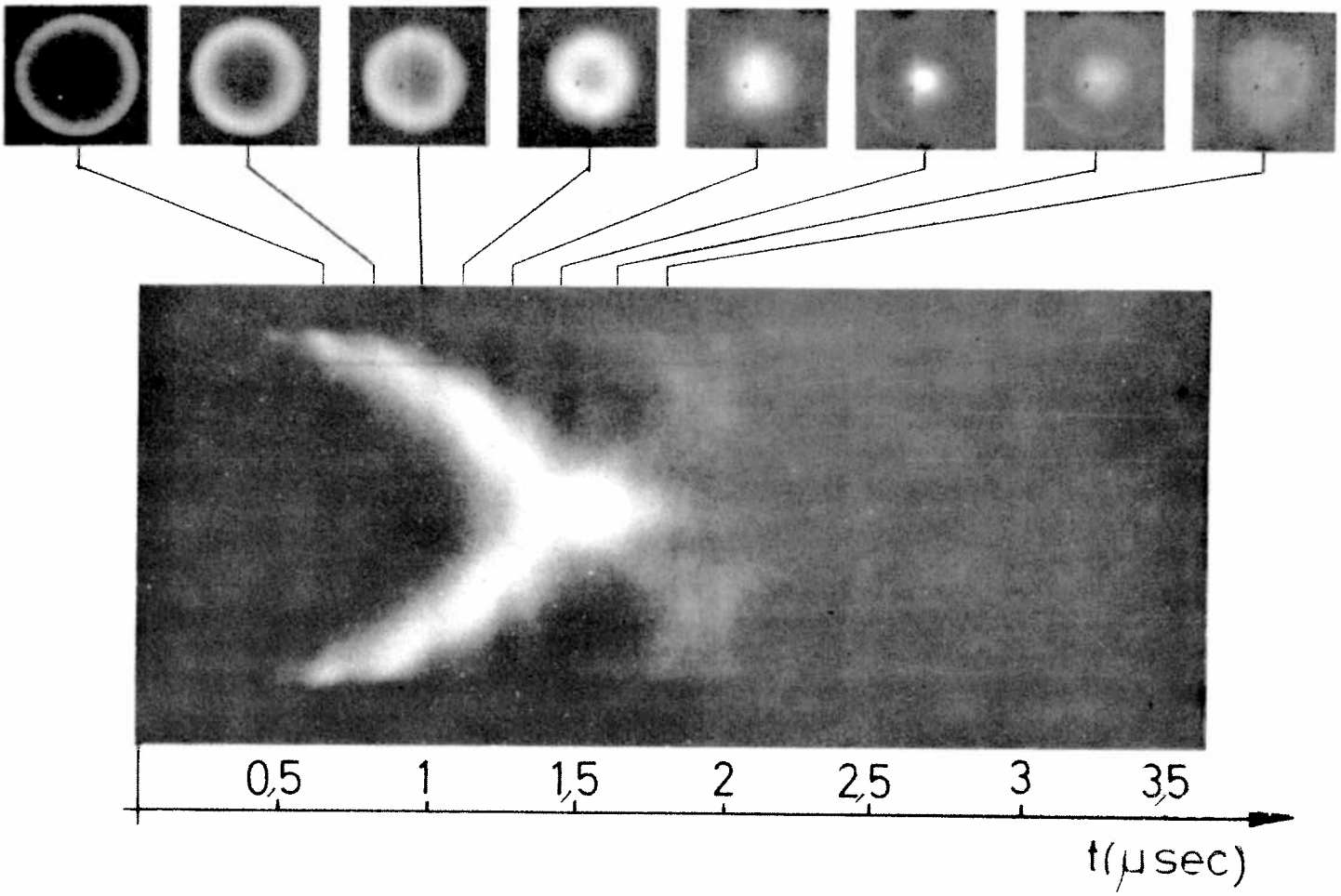

Fig. 3

STREAK AND FRAMING PHOTOGRAPHS OF A ROTATING FIELD PINCH (60m Torr He)

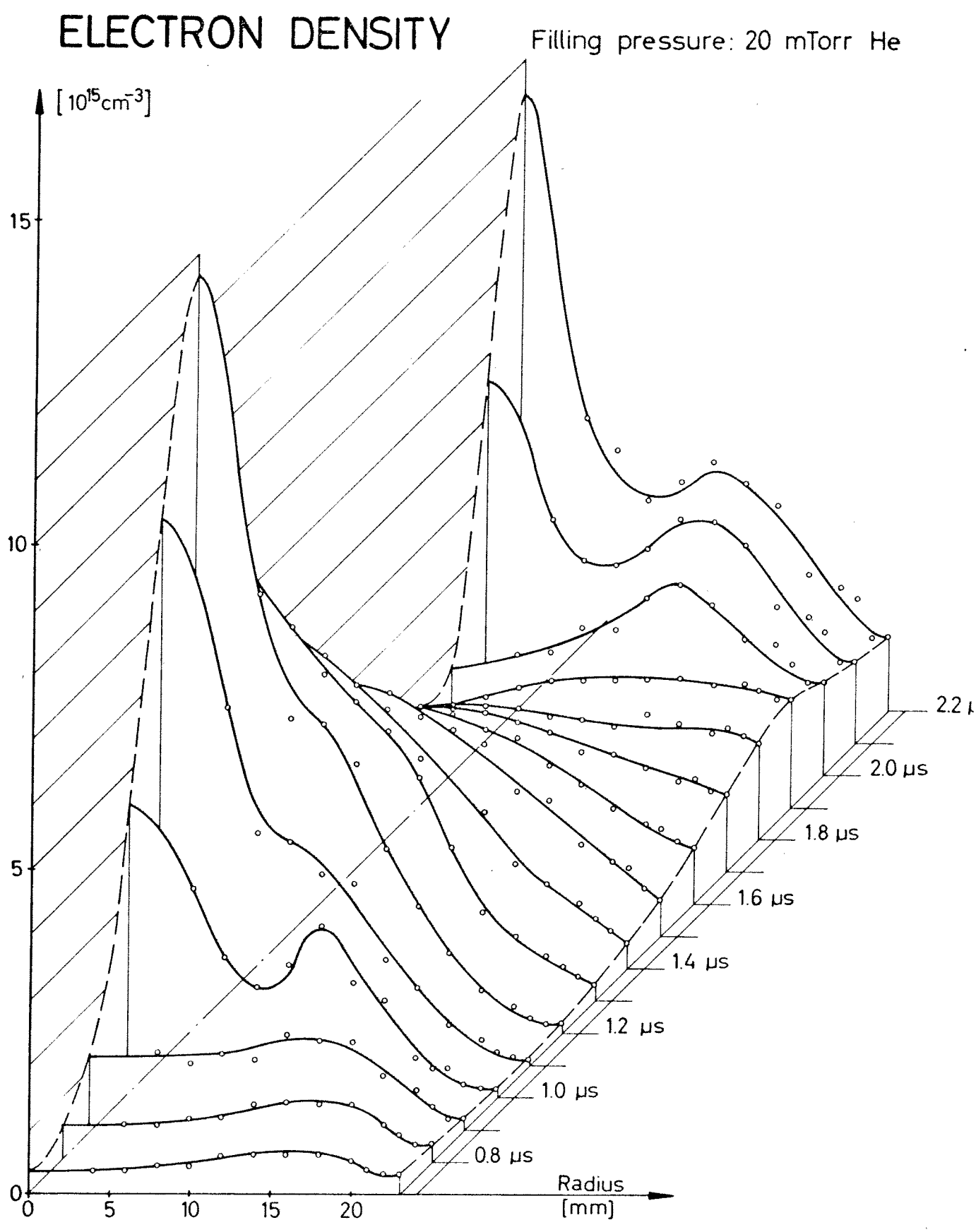
ELECTRON DENSITY
Filling pressure: 20 mTorr He
[10^15 cm^-3]
15
10
5
0
0
5
10
15
20
Radius
[mm]
0.8 µs
1.0 µs
1.2 µs
1.4 µs
1.6 µs
1.8 µs
2.0 µs
2.2 µ

FIG. 4

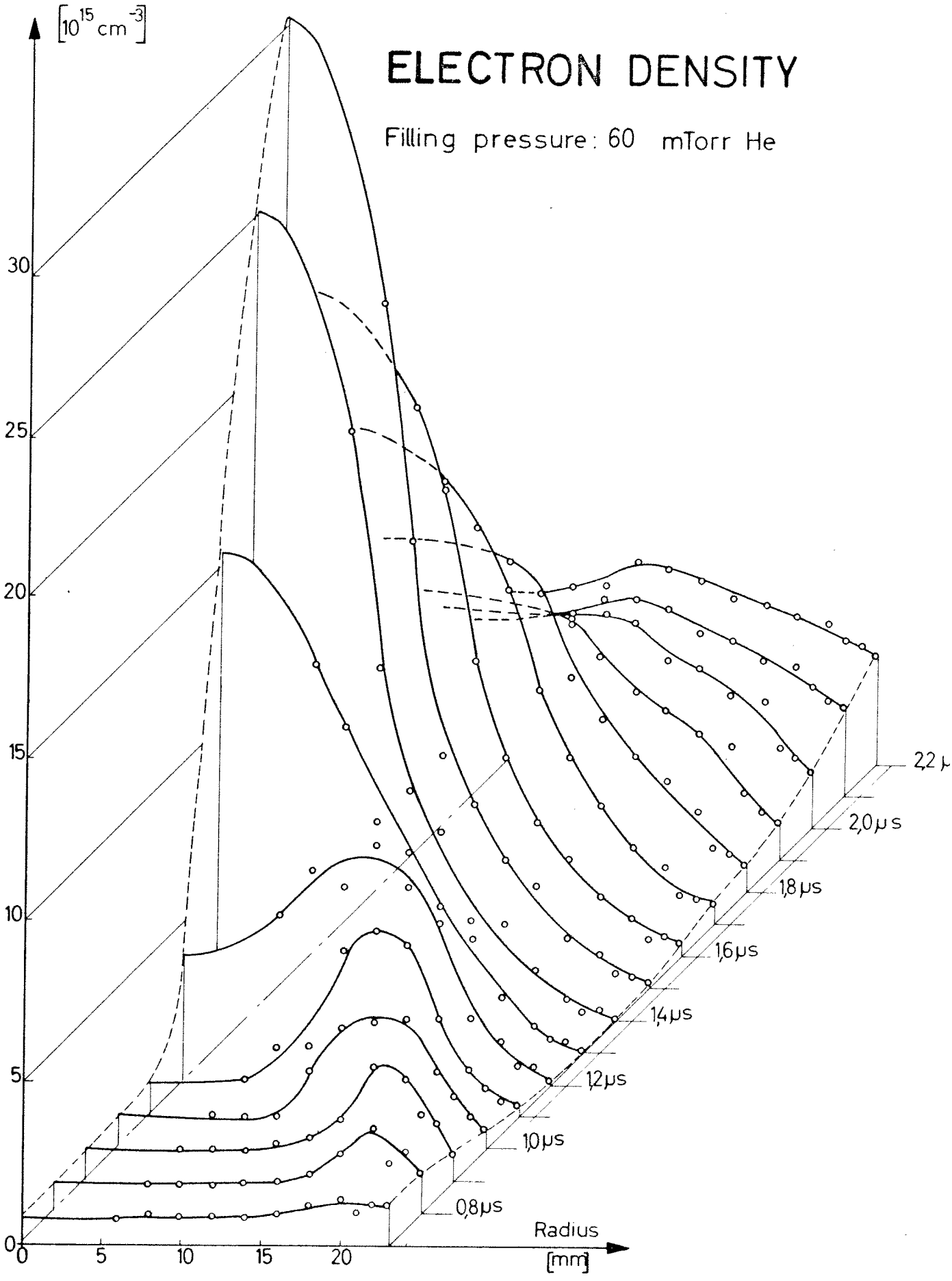
ELECTRON DENSITY
Filling pressure: 60 mTorr He
[10^15 cm^-3]
30
25
20
15
10
5
0
0
5
10
15
20
Radius
[mm]
0,8μs
1,0μs
1,2μs
1,4μs
1,6μs
1,8μs
2,0μs
2,2μ

FIG. 5

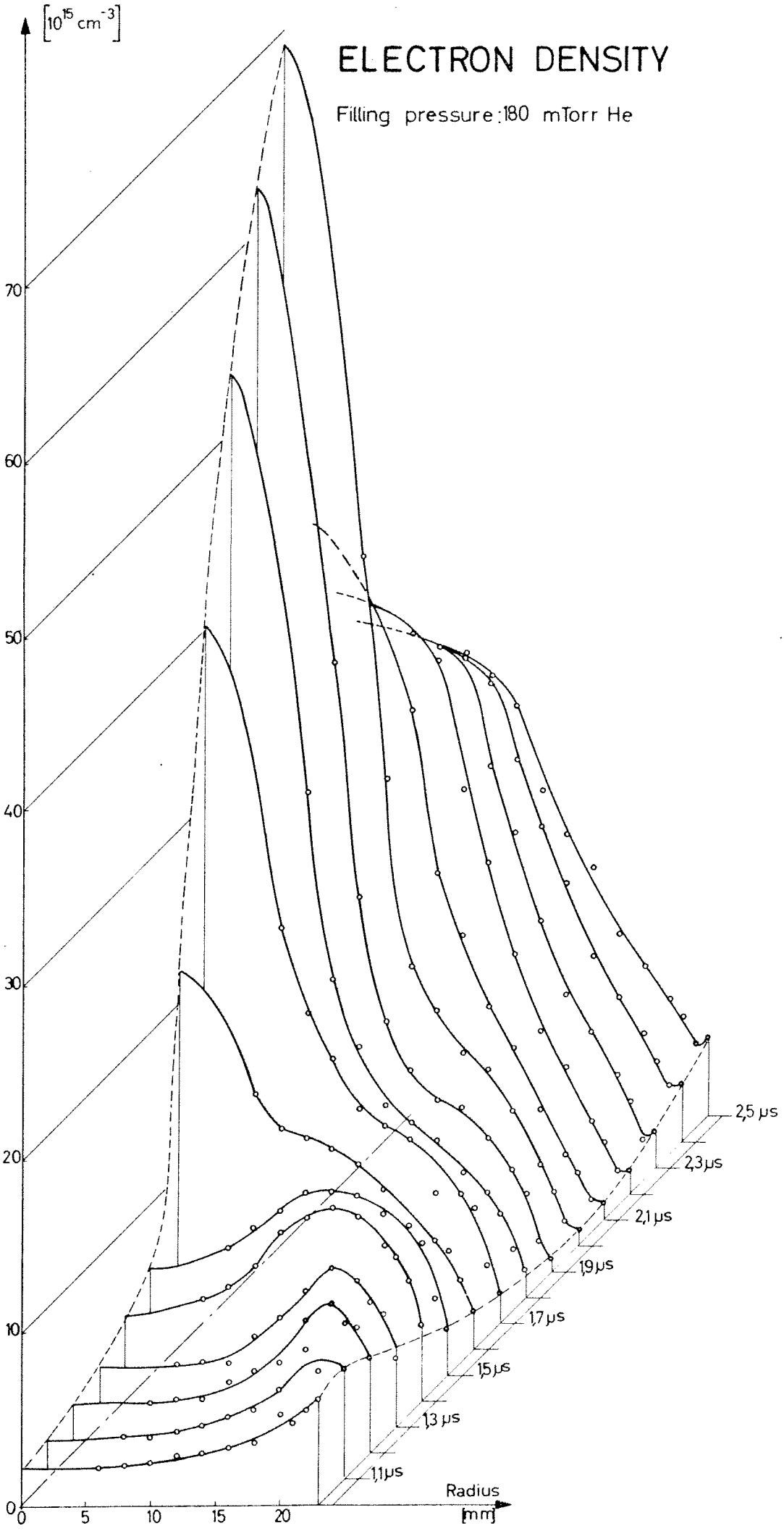
[10^15 cm^-3]
ELECTRON DENSITY
Filling pressure: 180 mTorr He
70
60
50
40
30
20
10
0
0
5
10
15
20
Radius
[mm]
2,5 µs
2,3µs
2,1 µs
1,9µs
1,7 µs
1,5µs
1,3 µs
1,1µs

FIG. 6

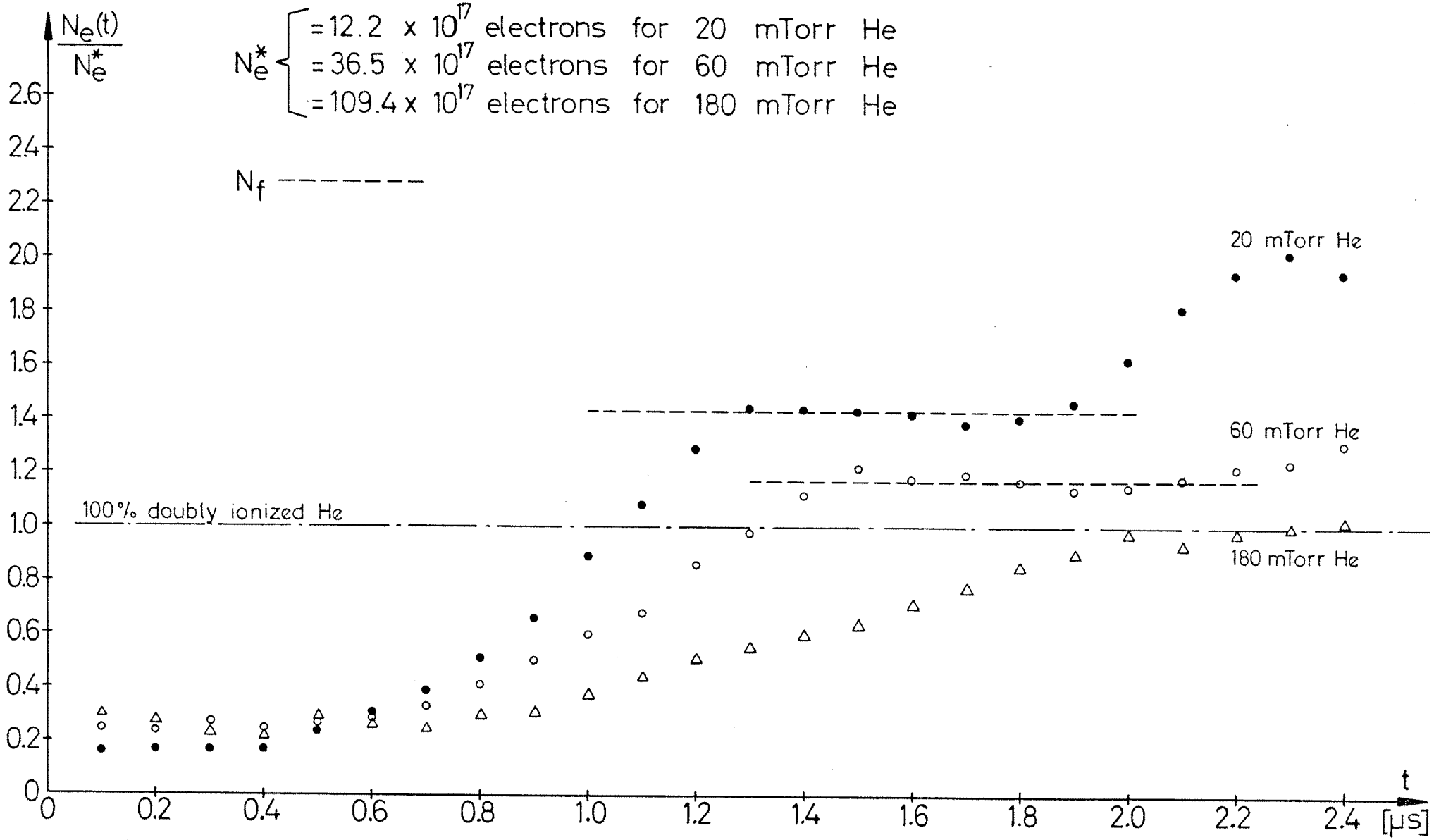

FIG. 7 TOTAL NUMBER OF ELECTRON . NORMALIZED

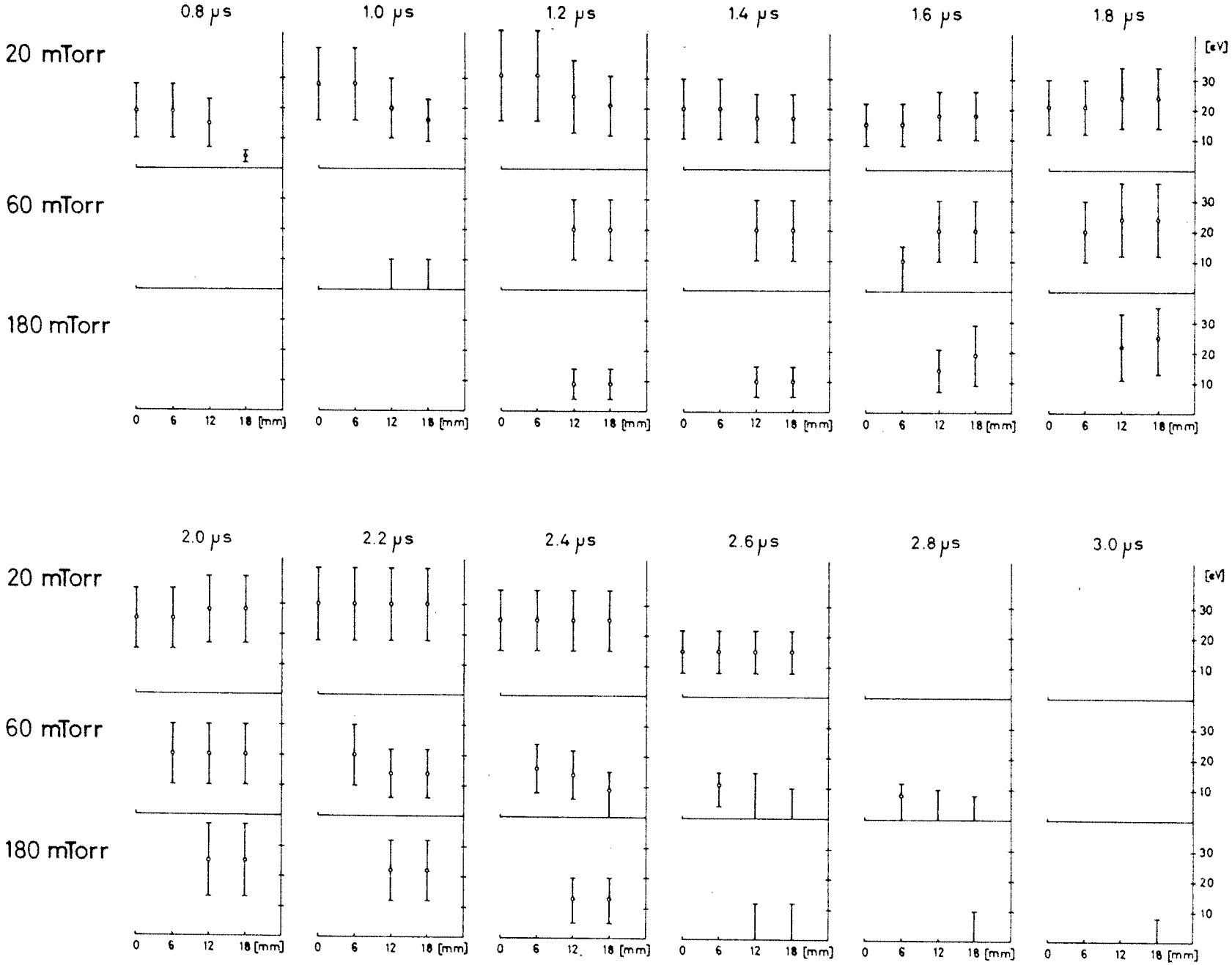

FIG. 9 — TEMPERATURE OF THE H^+ IONS

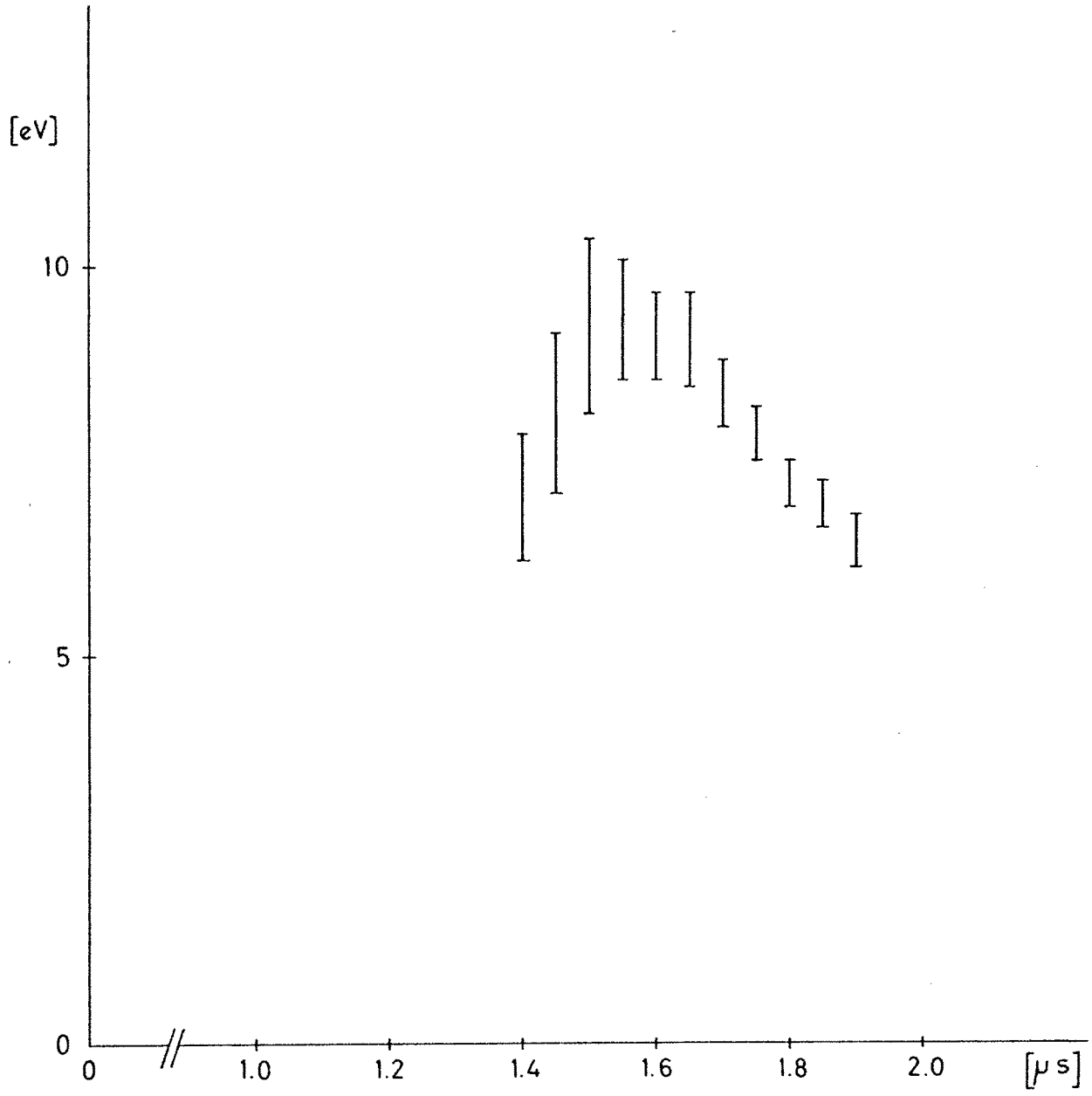

FIG. 9 ELECTRON TEMPERATURE

(60 mTorr He)

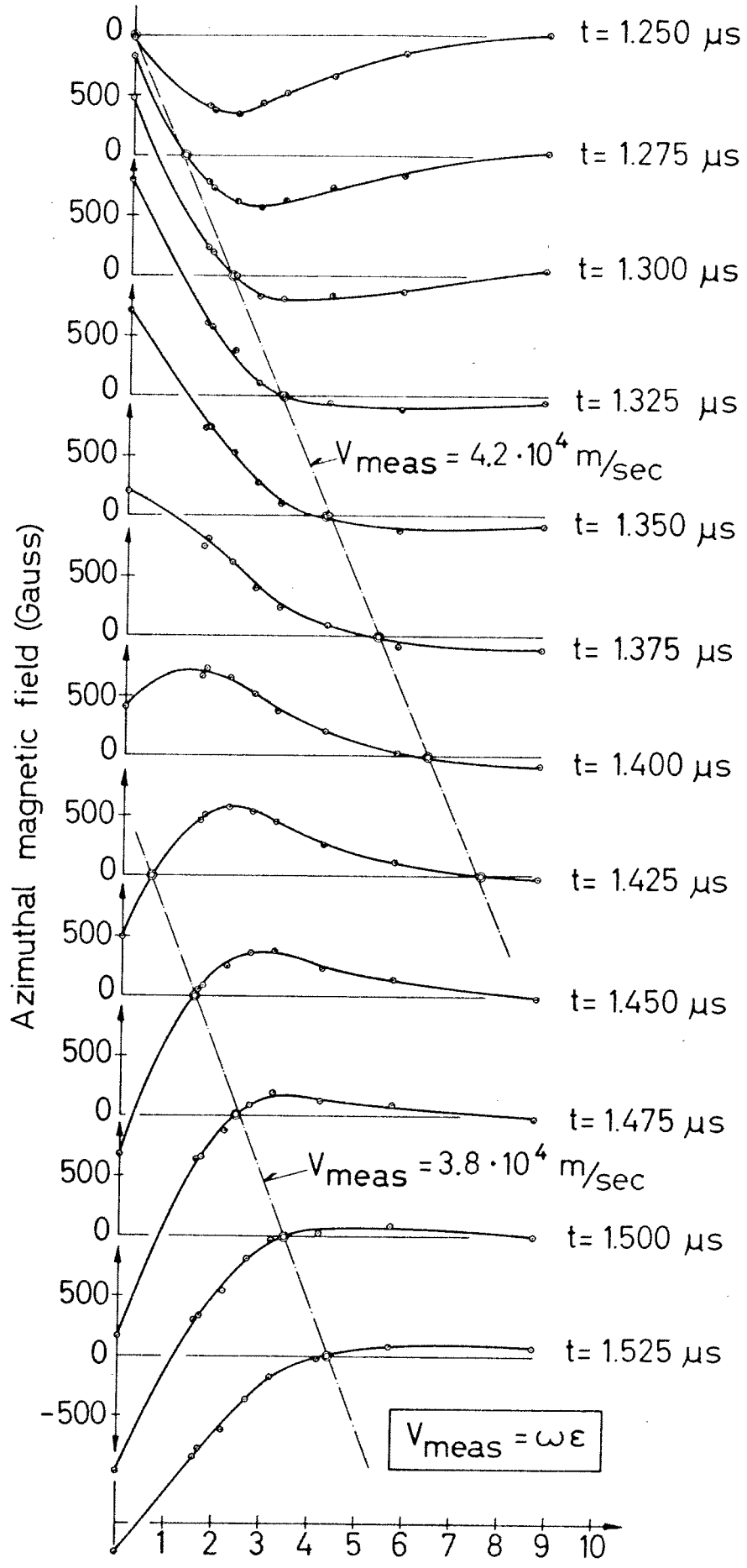

FIG. 10

RADIAL PROFILES OF AZIMUTHAL MAGNETIC FIELD AT VARIOUS TIMES (60 mTorr He)

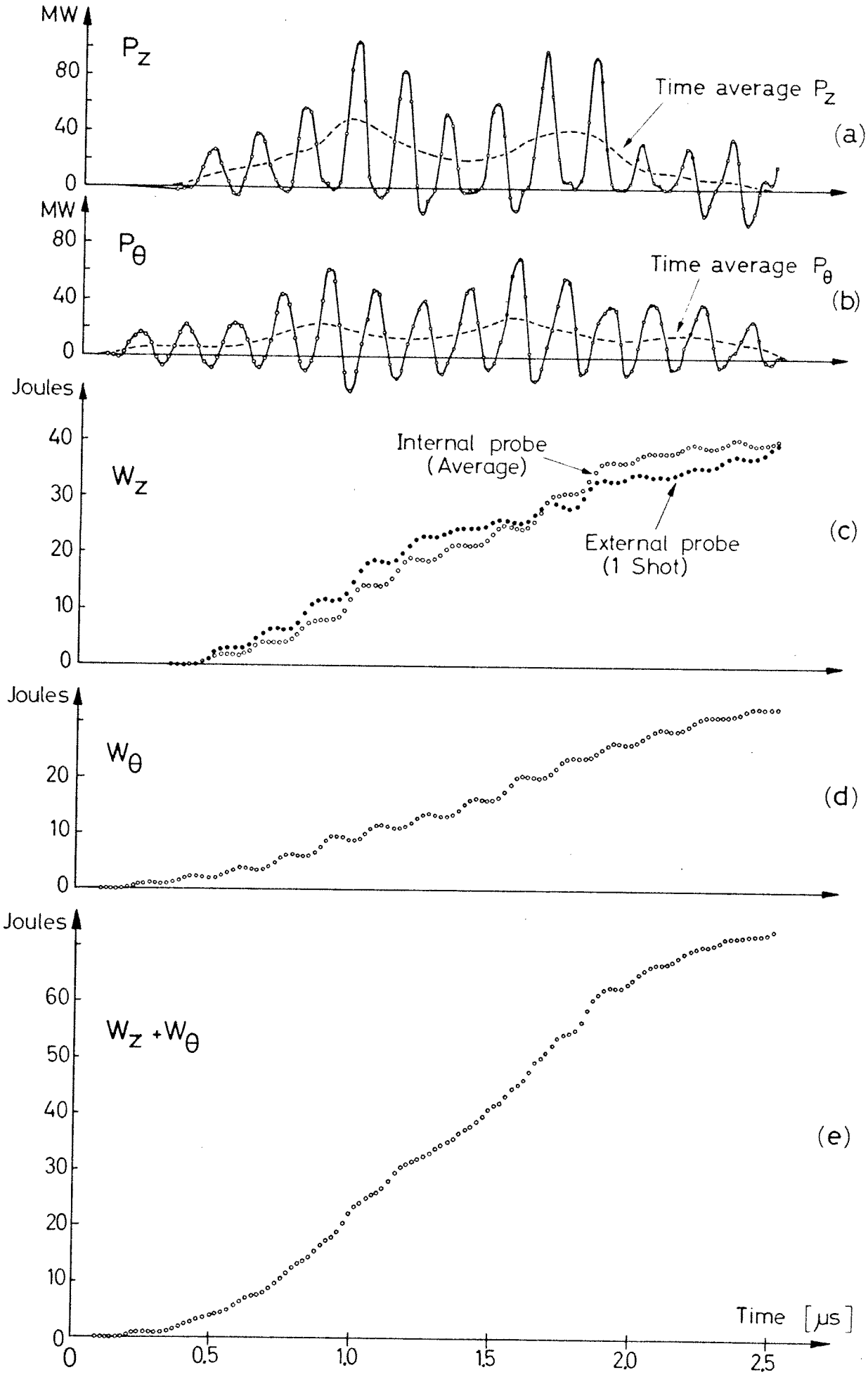

FIG. 11

POWER AND ENERGY
AS FUNCTIONS OF TIME
(60 mTorr He)

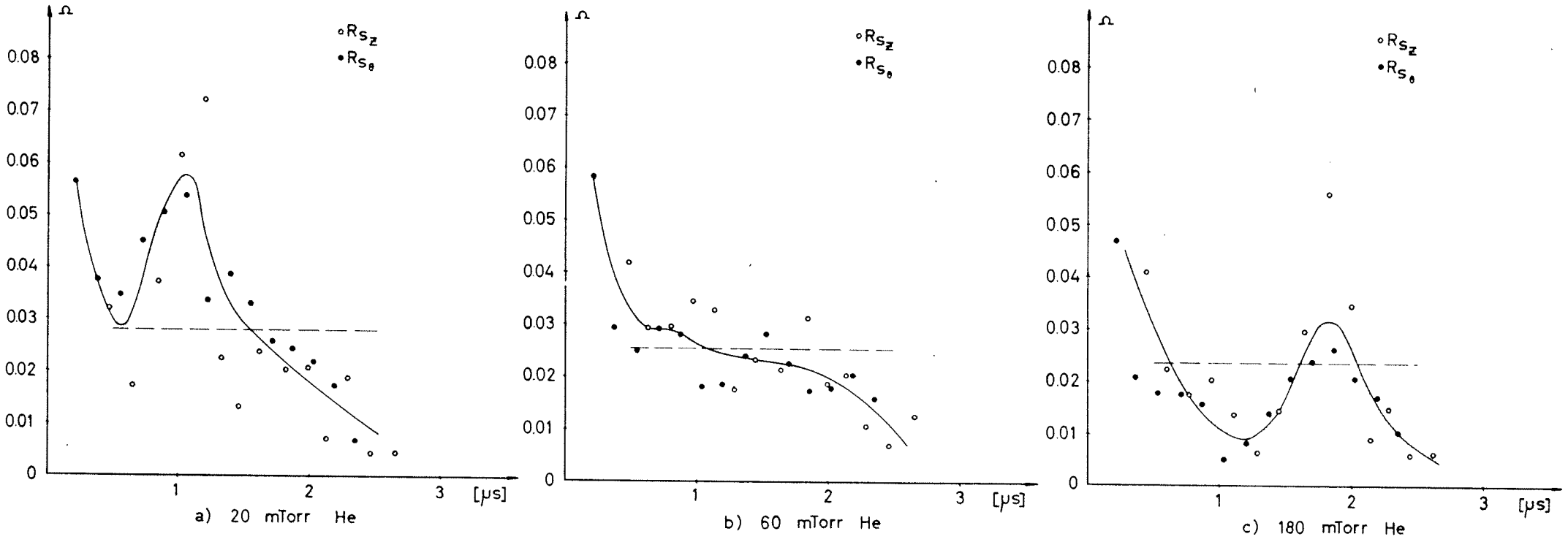

FIG. 12 VARIATION OF SURFACE RESISTIVITY, R_S, WITH TIME

– – – – Lietti's measurements (time average)

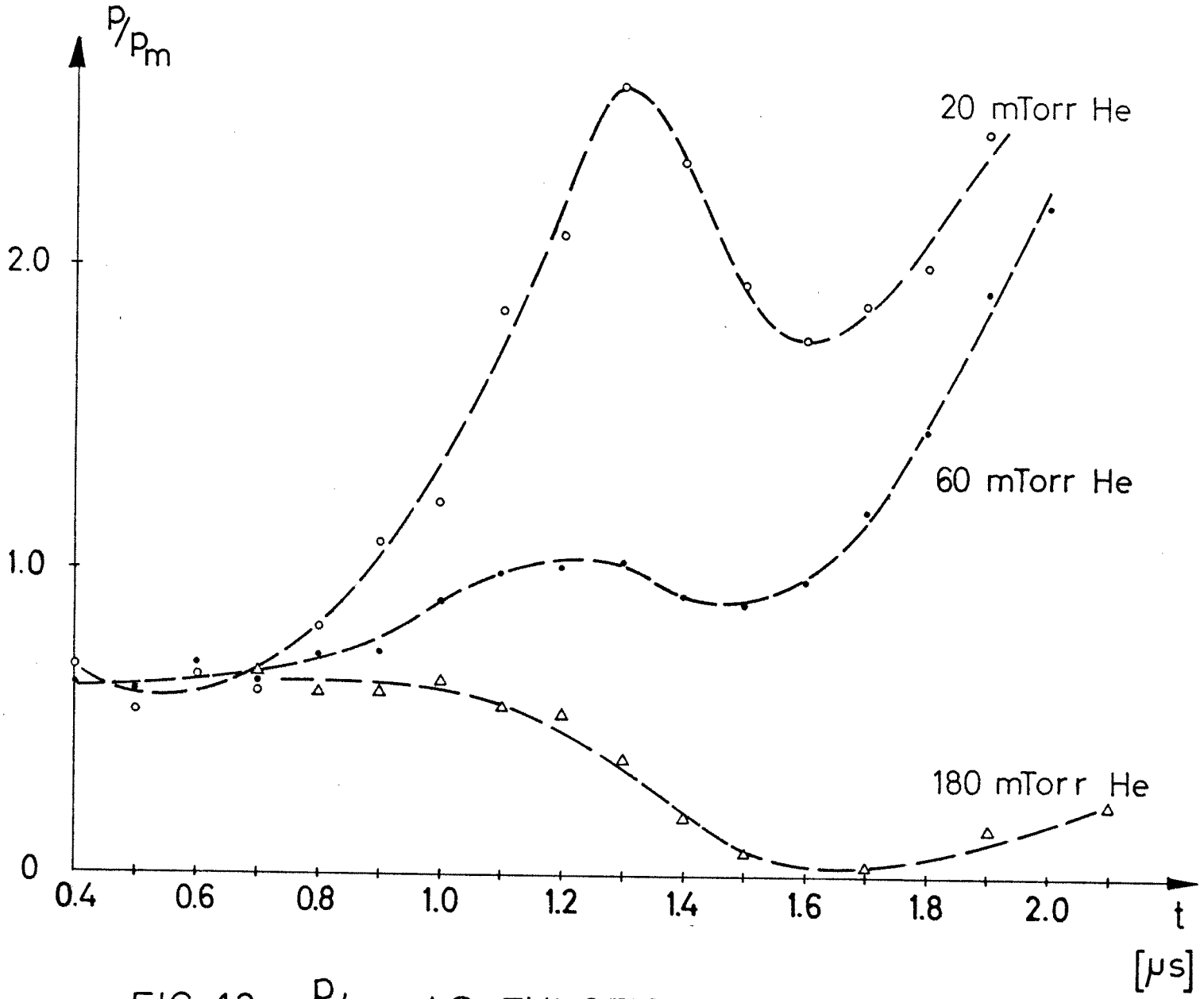

FIG. 13 p/p_m AS FUNCTION OF TIME

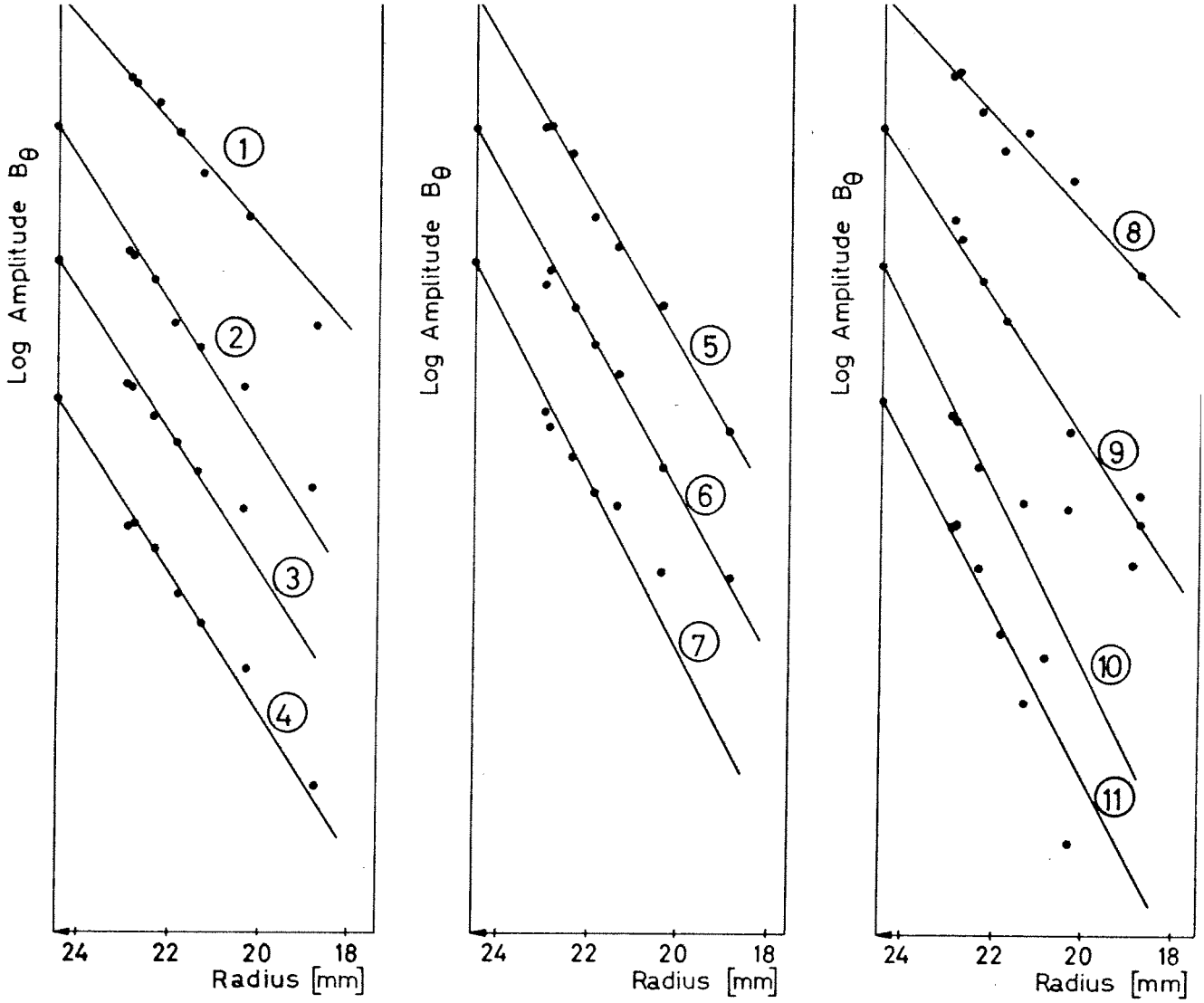

FIG. 14 VARIATION OF B_θ AMPLITUDE WITH RADIUS
Determination of δ at 60 mTorr He
(The numbers refer to successive maxima of B_θ)

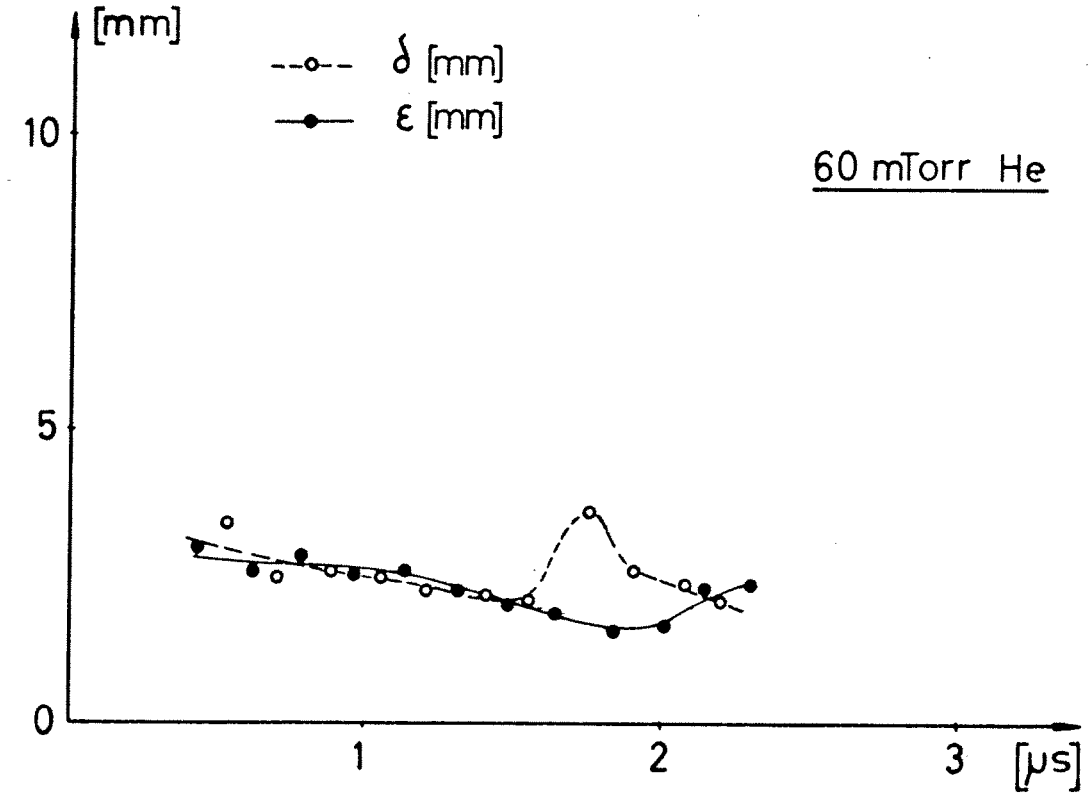

FIG. 15 VARIATION OF ε AND δ WITH TIME

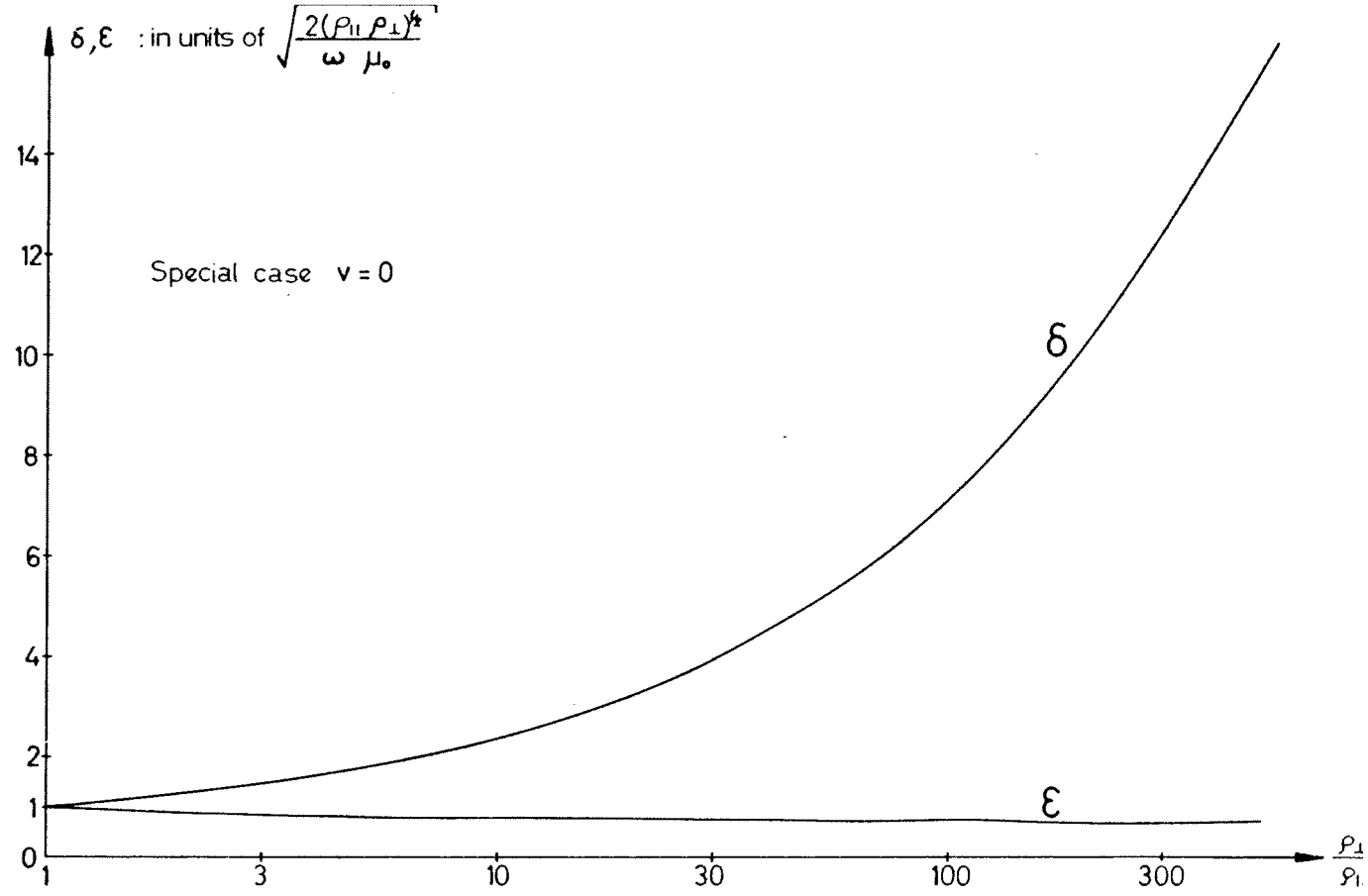

Fig.17 δ and ε as fonctions of the ratio $\frac{\rho_{\perp}}{\rho_{11}}$

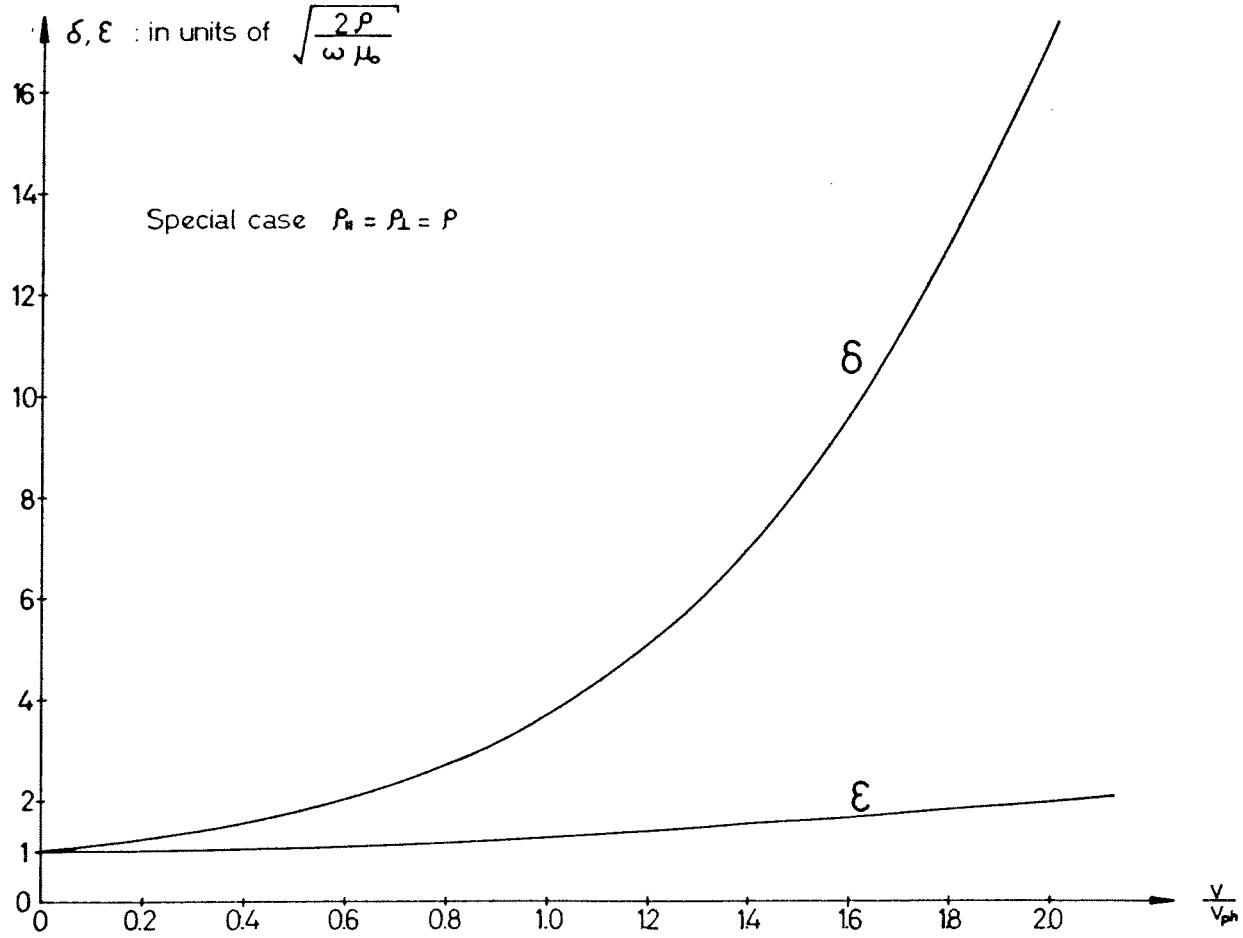

Fig.18 δ and ε as fonctions of the ratio $\frac{v}{v_{ph}}$

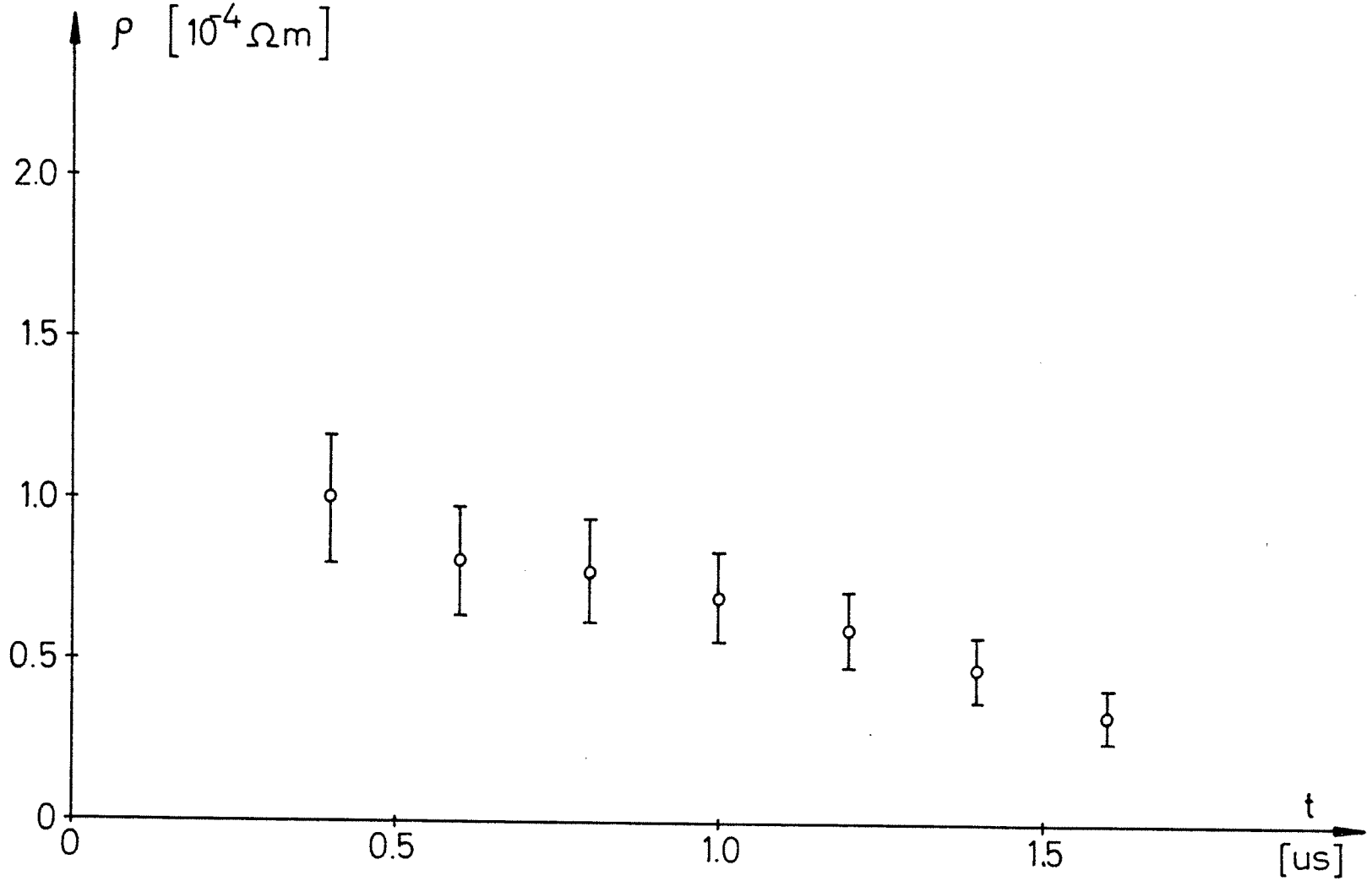

FIG.19 RESISTIVITY $\rho = R_S \delta$ (60 mTorr He)

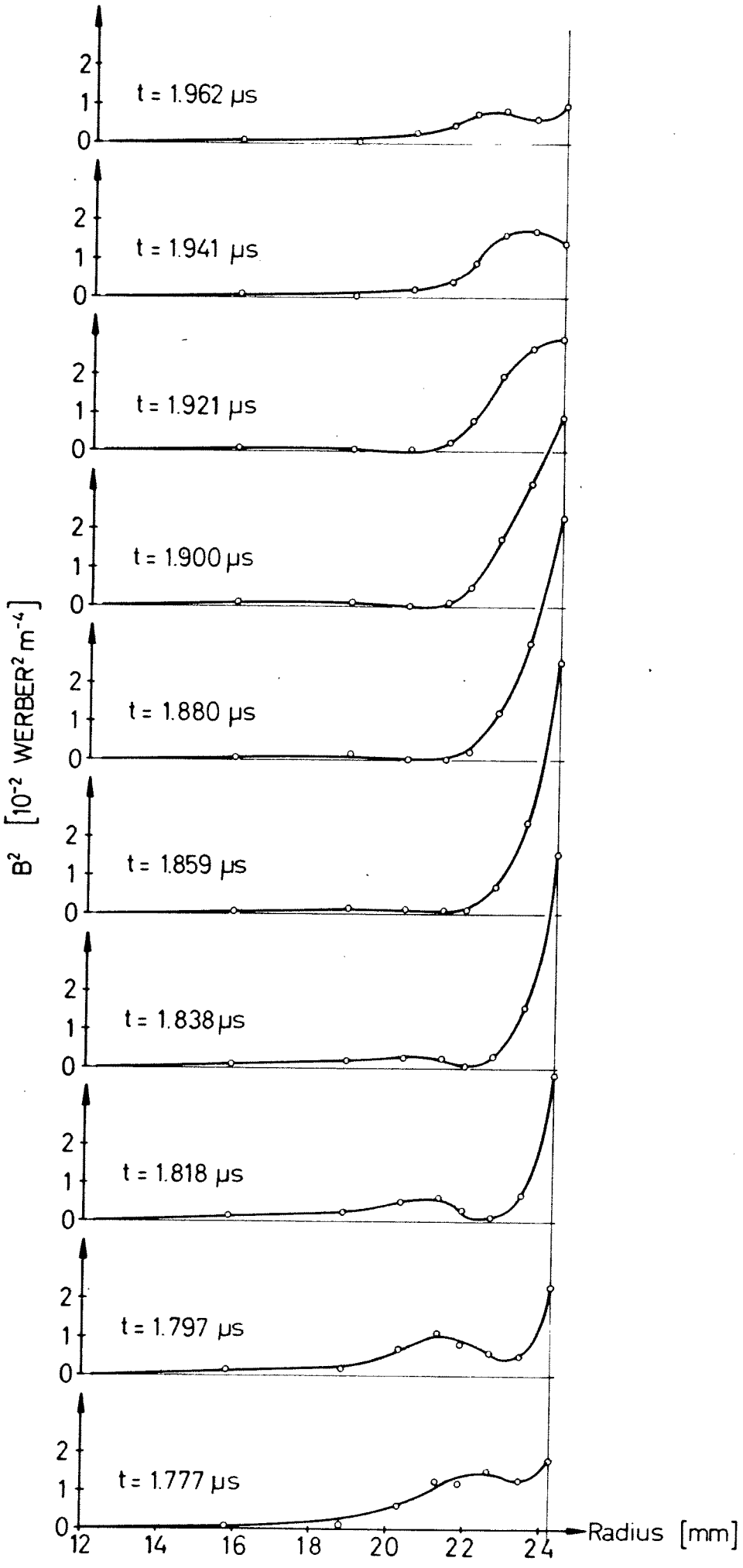

FIG.20 MAGNETIC PRESSURE
(60 mTorr He)